Effect of Anthropogenic Aerosols on Wheat Production in the Eastern Indo-Gangetic Plain

Shreemat Shrestha [1],*, Murray C. Peel [1], Graham A. Moore [1], Donald S. Gaydon [2], Perry L. Poulton [2] and Swaraj K. Dutta [3]

1   Department of Infrastructure Engineering, University of Melbourne, Parkville, Melbourne, VIC 3010, Australia
2   CSIRO Agriculture and Food, Queensland BioScience Precinct, St. Lucia, QLD 4067, Australia
3   Department of Agronomy, Faculty of Agriculture, Bihar Agriculture University, Sabour 813210, Bihar, India
*   Correspondence: shreemats@student.unimelb.edu.au or shreematshrestha@yahoo.com

Abstract: The Indo Gangetic Plain (IGP) is a food basket of South Asia and is considered a hotspot for air pollution due to persistently high emissions of anthropogenic aerosols. High levels of aerosols in the IGP not only affect the health of people but also the health of the natural system and the climate of the region. Aerosol effects on crop production in the IGP is an emerging area of interest for policymakers and the scientific community due to their possible effect on the food security and livelihood of millions of people in the region. To investigate the effect of anthropogenic aerosols on wheat production in the eastern IGP, we used a calibrated and validated Agricultural Production System Simulator (APSIM) model at nodes in Bangladesh, India and Nepal, 2015–2017. The effects of anthropogenic aerosols on wheat production were examined by running the APSIM model under three conditions: firstly, the condition with anthropogenic aerosols, using the observed meteorological data; secondly, the condition without anthropogenic aerosols, considering only the radiative effect of anthropogenic aerosols (adding the reduced radiation due to anthropogenic aerosols on the observed data); thirdly, the condition without anthropogenic aerosols, considering the radiation as well as temperature effects (by adding the reduced solar radiation and temperature due to anthropogenic aerosols on the observed data). The study revealed that, on average, anthropogenic aerosols reduced the wheat grain yield, biomass yield, and crop evapotranspiration by 11.2–13.5%, 21.2–22%, and 13.5–15%, respectively, when considering the 2015–2017 seasons at the target sites of eastern IGP. The study also showed an average reduction of more than 3.2 kg per capita per annum of wheat production in the eastern IGP due to anthropogenic aerosols, which has a substantial effect on food security in the region. Moreover, the loss of wheat grain yield due to anthropogenic aerosols in the eastern IGP is estimated to be more than 300 million USD per annum during the study period, which indicates a significant effect of anthropogenic aerosols on wheat production in the eastern IGP.

Keywords: APSIM; eastern IGP; wheat; aerosols; SRSFI; crop model

1. Introduction

The Indo Gangetic Plain (IGP) region of South Asia has become a hotspot for anthropogenic aerosol emissions, resulting in adverse impacts on the health and environment of the region [1,2]. Several studies based on satellite data and ground observations have depicted the IGP region as one of the most polluted regions of the world due to persistently high levels of atmospheric aerosols [3–6]. The high level of atmospheric aerosols in the IGP is not only due to anthropogenic emissions from one of the most densely populated regions of the world, but also due to the conducive conditions for concentrating aerosols created by the local topography and meteorology [7]. The spatial and seasonal variation in aerosols within the IGP is governed by aerosol sources, vertical and horizontal transport, and local and regional meteorology [8]. The average aerosol optical depth (AOD), a measure of the

proportion of sunlight that is extinguished before reaching the ground, of the entire IGP during 2006–2015 was 0.503, which is more than four times that of the global average [9]. In the eastern IGP, mainly eastern Uttar Pradesh, north and central Bihar, there were persistent periods of a high AOD of greater than 0.8 [5]. The major anthropogenic emissions in the IGP derive from fossil fuel combustions (vehicular and industrial emissions) and biomass burning (residential cooking and space heating and crop residue burning in the field) [10–12]. The major natural aerosols in the IGP are mineral dust transported from the Thar Desert and west Asian dry regions during pre-monsoon seasons and the sea salt brought from the Arabian sea and the Bay of Bengal [13,14]. The increasing trend of aerosols in recent decades in the IGP region is mainly due to the increased emissions of anthropogenic aerosols due to increased urbanization and industrialization [15–17]. Recently, in 2018, 16 cities of the IGP were listed as the 20 most polluted cities in the world based on mean annual particulate matter $PM_{2.5}$ concentration [18].

Air pollution remained a leading risk factor for death and disease burden in India in 2017 [19]. Total premature mortality due to exposure to ambient $PM_{2.5}$ in India is estimated to be 999,000 per year, with 24,606,000 years of life lost (YLL), of which the IGP region contributes 71 percent of the Indian total [20]. Along with the negative effects of atmospheric aerosols on the health of people in the IGP, serious effects are also reported on the natural systems of the region, which are mainly driven by changes in radiative forcing. Ramanathan and Ramana [21] studied radiative forcing due to atmospheric aerosols in the IGP during the dry season (October to May) from 2001 to 2003 and found that the average reduction in surface radiation was 32 ± 5 Wm^{-2}. Similarly, Ramachandran and Kedia [22] estimated the average annual radiative forcing at Kanpur (urban) and Gandhi College (rural) in the IGP from 2006 to 2008 as -35.46 and -36.24 Wm^{-2}, respectively. The radiative forcing due to aerosols at the eastern IGP stations of Silguri, Kolkata and Sundarban during winter in 2014/2015 was -39.3, -70.3 and -38 Wm^{-2}, respectively [23]. Similarly, Kumar et al. [5] estimated the radiative forcing due to atmospheric aerosols at Varanasi during winter (2014/15) in the range from -51 to -80 Wm^{-2}. These studies clearly indicate that atmospheric aerosols significantly reduce solar radiation in the IGP, which may affect the natural environment of the IGP.

The global decline in surface solar radiation (SSR) due to atmospheric aerosols, termed 'surface dimming', which occurred from 1950 to 1990 [24], reversed (or brightened) in most places by the end of 20th century, except in India, where surface dimming occurred at the rate of -8 Wm^{-2} decade^{-1} [25]. Singh et al. [26] analysed trends in solar radiation at four meteorological stations in central and northern India during 1960–2003 and found that all stations showed a surface dimming of from 1.5% to 3.4% per decade. By analysing pan evaporation data of 58 widely distributed stations over India during 1971 and 2010, Padmakumari et al. [27] concluded that there was a decreasing trend in pan evaporation at the rate of 9.24 mm per annum^2 with a statistically significant confidence level of 99.9 percent.

The expected impact of continued surface dimming on the Indian monsoon remains unclear. For example, reduced evaporation from the ocean, due to reduced solar radiation, may also reduce the moisture inflow to south Asia and weaken monsoon precipitation [28]. In addition to this, surface dimming in the IGP is suggested to be responsible for the weakening of the land–sea temperature gradient and result in a southward shift in the Asian monsoon circulation, decreasing its intensity [28]. Conversely, using the elevated heat pump (EHP) hypothesis, the increased loading of aerosols in the IGP during the pre-monsoon season may be responsible for the increased heating of the upper troposphere with the formation of an upper-level warm core anticyclone over the Tibetan Plateau from April to May, which may result in the advance of the monsoon into northern India and a subsequent increase in rainfall in the Indian sub-continent [29,30]. Recently, Frechet et al. [31] analysed the effect of local aerosols using numerical simulations (1982–2016) at the regional scale and found that the maximum temperature during winter is reduced by 0.5 °C in north-eastern India (eastern IGP), and precipitation is locally decreased by

0.5 mm day^{-1} over north India due to anthropogenic aerosols. Despite these different theories on the effect of aerosols on the summer monsoon, all these studies recognized that the occurrence and pattern of the monsoon is affected by high levels of atmospheric aerosols in the IGP region. Since the summer monsoon provides from 75 to 90 percent of precipitation in the IGP, the agricultural performance of the IGP is largely affected by the monsoon pattern and performance. High aerosol levels are also expected to affect other agriculturally relevant meteorological features in the region. Wide areas of the IGP, from Pakistan to Bangladesh, are engulfed by fog/low cloud during winter due to fine aerosols contributing to fog formation as cloud condensation nuclei [32]. Fog frequency in the IGP increased by 118.4% during 1971–2015 in the winter months of December and January [33]. Fog events negatively affect the growth and development of wheat due to a reduction in solar radiation availability, increased cold stress and favourable conditions for disease and pest [34]. It is believed that the increased aerosols in the IGP also indirectly affect crop production in the region through the change in natural systems viz. changes in monsoon precipitation, disease, pest population, water availability, etc. Along with those indirect effects, the reduced solar radiation, due to high levels of atmospheric aerosols, may also directly affect crop production in the IGP. In this context, studies related to the direct effect of atmospheric aerosols on crop production are discussed below.

Assessments of the effect of atmospheric aerosols on crop production are mainly performed via three types of studies viz. experimental, statistical model and process-based model studies. Experimental studies, using open-top field chambers, are mainly conducted to study the effect of air pollutants in gaseous form viz. O_3, SO_2, NO_2, etc. [35–38]. In a chamber study, Hirano et al. [39] studied the effect of particulate matter deposition on the leaf surface and found that it affects stomatal conductance, photosynthesis, and transpiration by shading, plugging the stomata and increasing the leaf temperature. Similarly, the accumulation of particulate matter and trace elements on vegetation is reported to be affected by air pollution level, rainfall and the passage of time [40]. Weerakody et al. [41], using natural and synthetic leaves in experiments on the accumulation of particulate matter, found that all three characteristics of leaves viz. leaf size, leaf shapes and leaf surface characteristics are influential in the capture and retention of particulate matter. In a recent experimental study on the effect of deposition of aerosols on rice leaves at New Delhi in the IGP by Mina et al. [42], they found that aerosols reduced the yield of rice (Basmati varieties). Experimental studies on the effect of aerosols on crop production mainly focus on the effect of gaseous aerosols and the deposition of particulate matter on leaves, not on the effect on crop production of atmospheric aerosols reducing surface solar radiation.

Statistical modelling has also been used to study the effect of atmospheric aerosols on crop production in India and China. Auffhammer et al. [43] used a statistical model of historical rice harvest in India, coupled with a regional climate scenario, to suggest that increased brown cloud and greenhouse gases reduced harvest growth in the last two decades. Similarly, using a statistical model, Burney and Ramachandran [44] concluded that the combined effect of climate change and short-lived climate pollutants (SLCPs) from 1980 to 2010 reduced wheat yield by up to 36% in India. Gupta et al. [45] analysed the impact of temperature and solar radiation (due to atmospheric aerosols) on wheat production through a regression analysis of data from 208 districts in India from 1981 to 2009 and found that every 1 °C increase in average daily maximum and minimum temperature tends to lower yield by 2–4% and 1% increase in solar radiation increases yield by about 1%. By using historical MODIS AOD data during 2001–2013, their study also indicated that a one standard deviation decrease in AOD is estimated to increase wheat yield by about 4.8% in India. Likewise, in China, various statistical modelling results have shown that reduced solar radiation due to increased atmospheric aerosols resulted in a decline in rice, wheat and maize production [46–48].

Process-based crop simulation models are also widely used to study the effects of atmospheric aerosols on crop production and to investigate different scenarios. Using the Crop Environment Resource Synthesis (CERES) 3.1 model, Chameides et al. [49] presented

a 1:1 relationship between change in solar irradiance and change in rice and wheat yield in China; they suggested that the yield of 70% of crop growth is reduced by from 5 to 30% due to the regional haze in China. Greenwald et al. [50] used a modified CERES crop model to study the influence of aerosols on rice, wheat and maize production under various atmospheric conditions. They also found that aerosols tend to decrease plant water stress by reducing soil evaporation and transpiration when crops are grown under rainfed conditions.

Along with the CERES crop model, the Agriculture Production System Simulator (APSIM) model [51] is also used to study the effect of atmospheric aerosols on crop production. The model has been widely and robustly tested in South Asian cropping systems [52]. Liu et al. [53] used a calibrated APSIM model to study the impact of air pollution on wheat yield in the North China Plain and found that the reduction in incoming solar radiation due to air pollution significantly affects wheat yield. Similarly, Xiao and Tao [54] studied detailed field experiment data from four stations in the North China Plain from 1980 to 2009 and used the APSIM to investigate the impact of changes in climate on winter wheat yield and found that the significant decline in solar radiation (at rates ranging from 0.06 to 0.15 MJm^{-2} $decade^{-1}$) over the past three decades reduced wheat yield by 3–12% across the stations. Likewise, Zhang et al. [55] also found that declining average daily sunshine hours (at the rate of 0.0239 h/season) in the North China Plain, due to increasing air pollution, resulted in a decline in wheat yield from 1979 to 2012.

APSIM has also been used in the North China Plain to investigate the impact of aerosols on maize production. Sun et al. [56] indicated a positive linear correlation between maize yield and sunshine hours (from silking to harvest stage) and the important role of radiation during the grain-filling stage for the final yield of maize. Similarly, by using a calibrated APSIM model, Xiao and Tao [57] found that changes in climate variables from 1981 to 2009 in the North China Plain reduced maize yield by from 15 to 30%. They also found that, among the changing climate variables, the highest reduction in maize yield 12–24% was due to the reduction in solar radiation (caused by increased atmospheric aerosols) during that period. Crop simulation modelling is an important tool for quantifying the effect of atmospheric aerosols on wheat and maize production in China.

The impact of aerosols on the natural system and crop production in the IGP is an emerging area of interest for policymakers and the scientific community. Studies on the effects of atmospheric aerosols on crop production in IGP are very important with respect to food security in this region, as this region produces 53% of rice and 93% of wheat produced in the IGP countries (Pakistan, India, Nepal, and Bangladesh) [58]. The IGP is home to about 800 million people spreads across four countries [59] and the negative effects of atmospheric aerosols on crop production could threaten the livelihoods of many people in this region. In the eastern IGP, the effect could be more serious because of the comparatively higher atmospheric aerosol levels and dominance of agriculture by smallholders (with low risk-bearing capacity). Of particular interest is the impact of relatively high levels of aerosols during winter in the eastern IGP [5,60,61] and their effect on the performance of the major winter crop, wheat. Some studies based on statistical models [43–45] have shown a significant negative effect of atmospheric aerosols on crop production (rice and wheat) in India. However, studies on the effects of atmospheric aerosols in the IGP using process-based models in the IGP are lacking. In this context, this study aimed to investigate the effect of atmospheric aerosols on winter wheat production in the eastern IGP using a calibrated APSIM model. This study also intended to quantify the economic implications of the impact of air pollution on winter wheat production in the IGP to inform policymakers about the potential benefits of pollution control programs in the region.

2. Materials and Methods

2.1. Study Area

The IGP is one of the largest fertile plains in the world formed by the Indus and Ganges river systems, and it encompasses the eastern plain area of Pakistan, most of northern and

eastern India, the southern plain area of Nepal and almost all of Bangladesh. The IGP is home to 1 billion people, and it is also the 'food basket' of the region, producing 53% of rice and 93% of wheat of those countries [58]. Considering biophysical conditions and socioeconomic development, the IGP can be divided into two broad categories: western IGP and eastern IGP [59]. Our study area is the eastern IGP, which encompasses Bihar and West Bengal of India, the eastern Terai area of Nepal and the plain area of Bangladesh (Figure 1).
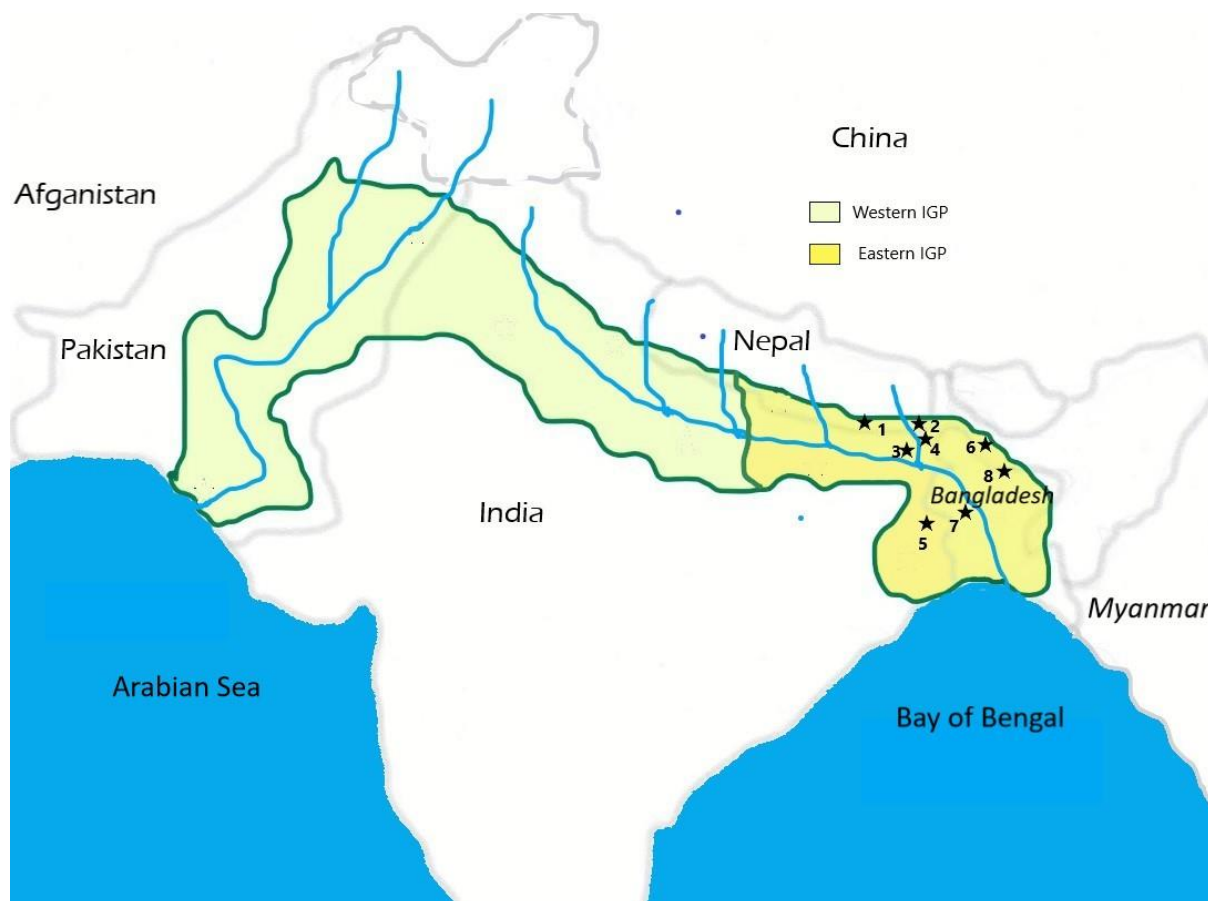
Figure 1. Study area, the eastern IGP and the Sustainable and Resilient Farming Systems Intensification (SRSFI) project districts (1—Dhanusha and 2—Sunsari of Nepal; 3—Madhubani and 4—Purnea of Bihar, India; 5—Cooch Behar and 6—Malda of West Bengal, India; and 7—Rajshahi and 8—Rangpur of Bangladesh).

The biophysical and socio-economic characteristics of the eastern IGP are different from the western IGP. There is a clear gradient in annual average precipitation in the IGP, ranging from 654 mm in Punjab (western IGP) to 1462 mm in West Bengal (eastern IGP) [62]. The climate of the eastern IGP is hot and sub-humid with a monsoon season (June to September), in which about 85% of total precipitation occurs [63]. Despite the higher precipitation in the eastern IGP, compared to western IGP, crop productivity in the eastern IGP is lower due to a lack of assured irrigation facilities, low levels of agricultural input, traditional agriculture systems and climate extremes (flood and droughts) [59]. A major characteristic of the eastern IGP is low-lying flood-prone land, formed by alluvium deposits from the Ganga river system [64]. The average land-holding in the eastern IGP is small (only 0.59 ha/household) and less mechanized compared to the western IGP (3.55 ha/household) [65]. The IGP is considered to be one of the most densely populated regions of the world, with a population of more than 800 M [59] and a clear gradient (ascending) of population density from west to east [62]. Census data from 2011 indicate

a total population of eastern IGP of more than 360 million with an average population density of 991 people per square kilometre.

Increasing urbanization and high population density, industrialization and the dominance of biomass in domestic energy use has resulted in high levels of atmospheric aerosol loading in the IGP [1]. The persistence of an exceptionally high AOD (greater than 0.8) in eastern Uttar Pradesh, north and central Bihar is an important feature of aerosols in the eastern IGP, which are mainly due to emissions from households and industries, as well as local topography and meteorology acting to concentrate aerosols [5].

Rice is the most important crop of the eastern IGP, and the major seasonal cropping patterns of this region are rice–rice, rice–maize, and rice–wheat. Wheat is an important winter crop in Bihar, covering 2.1 M ha (47% of the net cropped area), whereas only 0.32 M ha (only 6% of the cropped area) is cultivated in West Bengal [66]. Similarly, wheat is also an important winter crop of the Terai area of Nepal, cultivated in 0.43 M ha (about 33% of the cropped area) [67]. In Bangladesh, rice covers more than 75% of the major cropping area cultivated in all three seasons—Kharif 1 (Aus rice), Kharif (Aman rice) and Rabi (Boro rice). Wheat and maize are the important Rabi crops after Boro rice in Bangladesh. In Bangladesh, wheat-cultivated area significantly declined after 1998/1999 as farmers preferred to cultivate maize due to the increased economic return of maize, higher productivity of hybrid maize (5.3 t/ha) compared to wheat (1.6 t/ha) and increasing demand for maize from the expanding poultry industry [68].

The Sustainable and Resilient Farming Systems Intensification (SRFSI) project is an Australian Centre for International Agricultural Research (ACIAR) and Australian Department of Foreign Affairs and Trade (DFAT) funded regional project implemented from 2014 to 2018 in the eastern IGP aims to reduce poverty by improving the productivity, profitability and sustainability of small farmers while safeguarding the environment [69]. The SRFSI Project focusses on the eastern IGP of Bangladesh, India, and Nepal and has established 40 nodes/villages across eight districts (Figure 1) to implement project activities. One project activity conducted at these 40 nodes was on-farm trials to compare conservation agriculture technologies with conventional tillage practice. After checking data quality, on-farm trials at two nodes at each district of Rajshahi, Rangpur, Purnea, and Sunsari were selected for SRFSI on-farm calibration and evaluation of the APSIM crop simulation model. The details of those nodes are presented in Table 1. In all nodes, APSIM was set up to simulate the rice-wheat cropping system, but, in this study, only the winter wheat crop was analysed.

Table 1. Details of nodes in which the SRFSI on-farm APSIM calibration and validation was conducted based on on-farm experimental trials [70].

Country	District	Nodes	Latitude	Longitude	Cropping System Simulated
Nepal	Sunsari	Simariaya	26.570	87.239	Rice-wheat
		Bhaluwa	26.547	87.249	Rice-wheat
India	Purnea	Dogachi	25.516	87.334	Rice-wheat
		Tikapatti	25.312	87.124	Rice-wheat
Bangladesh	Rajshahi	Baduria	24.337	88.717	Rice-wheat-mung bean
		Premtoli	24.406	88.434	Rice-wheat
	Rangpur	Kolkondo	25.875	89.199	Rice-wheat-jute
		Mohonpur	25.375	88.875	Rice-wheat-jute

The monthly mean maximum and minimum temperature and the precipitation of the study districts from 2014 to 2016 are shown in Figures 2 and 3, respectively. The monthly maximum and minimum temperature indicate that the study district Rajshahi is

comparatively warmer and Sunsari is comparatively cooler. All four study districts show a similar precipitation pattern, with precipitation mainly being concentrated in the monsoon period and only nominal winter precipitation during the wheat-growing period.
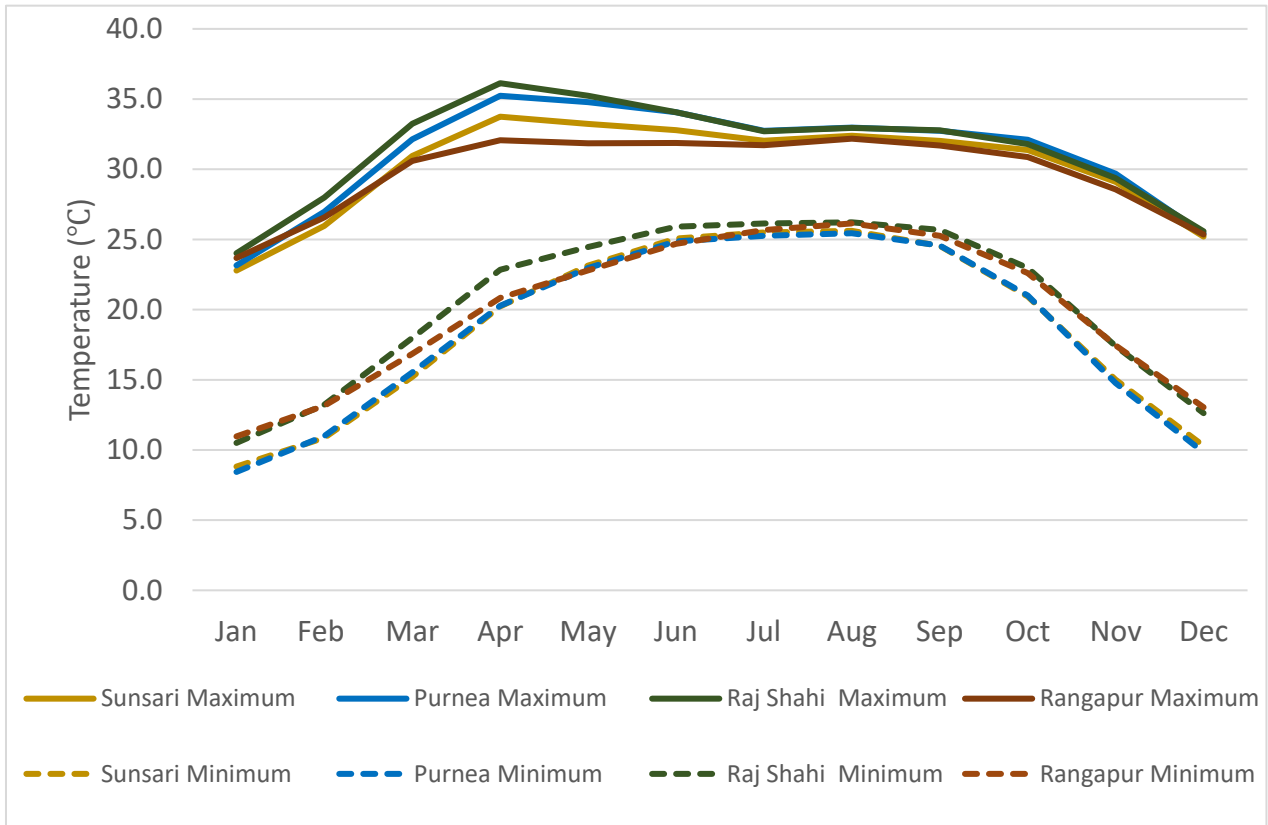
Figure 2. Monthly mean maximum and minimum temperature of the study districts.
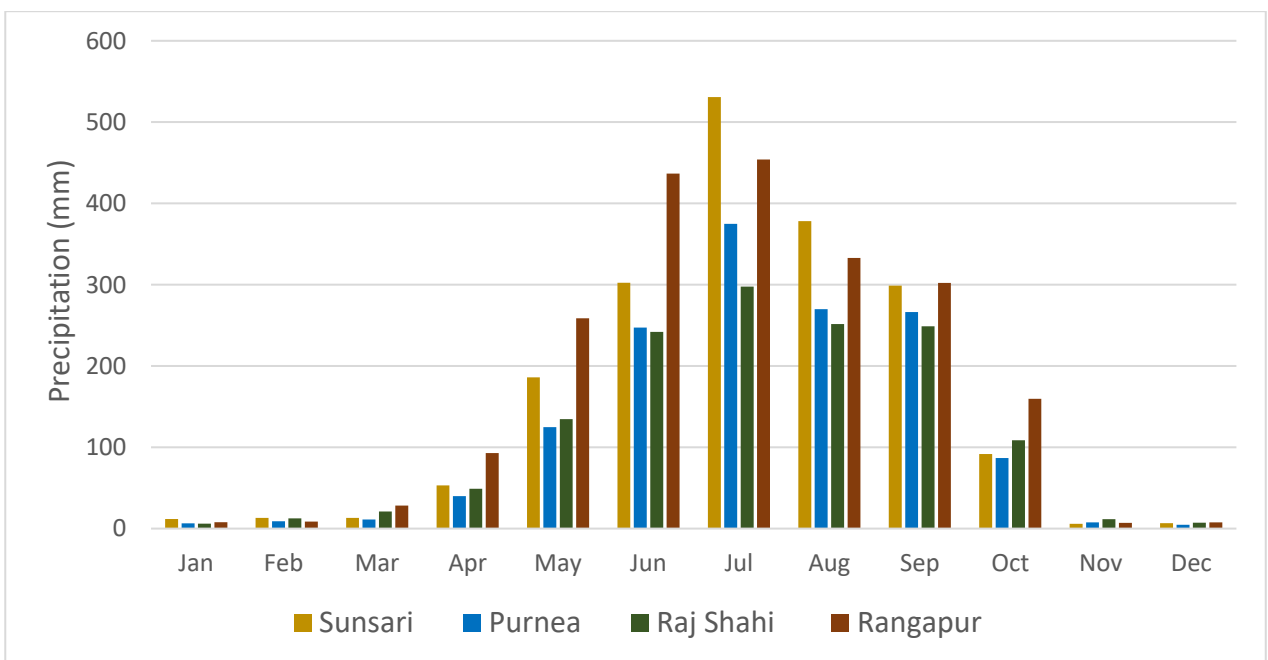
Figure 3. Monthly mean precipitation of the study districts.

2.2. Methods

2.2.1. Atmospheric Aerosols in the Eastern IGP

Atmospheric aerosols in the eastern IGP were studied using AOD at 500 nm and Angstrom exponent data from 2003 to 2017 at four AErosol RObotic NETwork (AERONET) stations (Lumbini, Gandhi college, Dhaka, and Bhola) located in the eastern IGP. The average monthly AOD and Angstrom exponent was calculated at each station to study the overall seasonal status of aerosols at those stations. To obtain historical AOD data at the SRFSI nodes listed in Table 1, area average daily MODIS Aqua AOD at 550 nm was extracted for pixels lying within $\pm 0.1°$ co-ordinates of each node from 2003 to 2017. The trend analysis of AOD at the SRFSI nodes was performed using a Mann–Kendall test [71]. A positive aspect of this method is that missing values are allowed, and data do need not to belong to any specific distribution. In addition, this method is robust to single data errors and outliers [72]. In this method, the trend is assumed to be monotonic and the equation for AOD as a function of time (years) is given by

$$f(t) = Qt + B \tag{1}$$

where Q is the slope and B is a constant.

2.2.2. Estimation of Radiative Forcing Due to Aerosols at SRFSI Nodes in Eastern IGP

There are direct and indirect effects of atmospheric aerosols on the energy balance of the earth–atmosphere system. The direct effects are derived through the scattering and absorption of solar radiation by aerosols in the atmosphere and the indirect effects are caused by aerosols acting as cloud condensation nuclei and modifying cloud properties (viz. albedo, lifetime, precipitation efficiency, etc.) [73]. The effect of the aerosols is measured in terms of radiative forcing, which is defined as the net radiative flux either at the bottom (surface of the earth) or top of the atmosphere with and without aerosols in the atmosphere [74]. Here, we are interested in the direct effect of atmospheric aerosols on incoming solar radiation at the surface of the earth. The direct radiative forcing at the surface (ADRF$_{clr}$) under clear sky conditions is expressed as Equation (2).

$$ADRF_{clr} = F_{clr}^{a\downarrow} - F_{clr}^{o\downarrow} \tag{2}$$

where

$F_{clr}^{a\downarrow}$ = Net downward flux with aerosol under clear-sky conditions;
$F_{clr}^{o\downarrow}$ = Net downward flux without aerosol under clear-sky conditions.

Clouds in the atmosphere also affect the energy balance of the earth–atmosphere system. Cloud radiative forcing is used to measure the impact of clouds on radiation and is defined as the difference between the clear-sky and all-sky radiation [75]. Liu et al. [76] derived a simple relationship for cloud radiative forcing with cloud albedo (α) and cloud fraction (f). Using this relationship, the incoming solar radiation at the bottom of the atmosphere without atmospheric aerosol ($F_{all}^{o\downarrow}$) can be expressed in terms of incoming radiation under clear-sky conditions using Equation (3).

$$F_{all}^{o\downarrow} = (1 - \alpha f)F_{clr}^{0\downarrow} \tag{3}$$

where

$F_{all}^{o\downarrow}$ = Net downward flux without aerosol under the all-sky condition.

If we assume no interaction between the clouds and aerosols in the atmosphere, the incoming solar radiation at the bottom of the atmosphere with atmospheric aerosols ($F_{all}^{a\downarrow}$) can also be expressed as analogous to the [76] relationship, as in Equation (4).

$$F_{all}^{a\downarrow} = (1 - \alpha f)F_{clr}^{a\downarrow} \tag{4}$$

The radiative forcing at the surface (ARF_{all}) in the all-sky condition is the difference between the net downward radiative flux all-sky condition with aerosols in the atmosphere ($F_{all}^{a\downarrow}$) and that without aerosols ($F_{all}^{o\downarrow}$) From Equations (2)–(4), the relationship between the all-sky radiative forcing (ARF_{all}) and clear-sky radiative forcing $ADRF_{clr}$ can be expressed as in Equation (5).

$$ARF_{all} = (1 - \alpha f)ADRF_{clr} \tag{5}$$

In this study, the clear-sky daily radiative forcing at the surface of the SRFSI nodes in the eastern IGP is estimated from a regression model (Equation (6)) developed by Shrestha et al. [77]. The input parameters of this model are the daily average atmospheric aerosol optical depth at wavelength 550 nm (AOD_{550}) and daily mean atmospheric water vapor (AWV). Daily merged dark target (DT) and deep blue (DB) AOD products and daily mean atmospheric water vapor from MODIS Aqua were extracted for pixels lying within $\pm 0.1°$ of the SRFSI nodes listed in Table 1 for the years from 2014 to 2017.

$$ADRF_{clr} = -32.464 - 119.446 * AOD_{550} + 4.471 * AWV \tag{6}$$

The area-averaged cloud albedos at pixels within $\pm 0.1°$ of the SRFSI nodes listed in Table 1 were extracted from the Modern-Era Retrospective analysis for Research and Applications, version 2 (MERRA-2) for the same duration. Similarly, the area-averaged mean daily cloud fraction at pixels within $\pm 0.1°$ of the SRFSI nodes were obtained from MODIS Aqua for the years from 2014 to 2017. The daily direct radiative forcing at the surface under all-sky conditions (ARF_{all}) for the SRFSI nodes listed in Table 1 during 2014 and 2017 was computed using Equation (5).

The radiative forcing estimated from Equation (5) provides the radiative forcing at the surface by aerosols from both natural and anthropogenic sources. Here, we are interested in the radiative forcing due to anthropogenic aerosols. In the IGP region, anthropogenic and natural aerosols exhibit distinct seasonal characteristics and mixing [5,7,22,78,79]. Dey and Tripathi [80] studied radiative forcing due to atmospheric aerosols and the anthropogenic contribution on a monthly basis at Kanpur in the IGP and found that anthropogenic aerosols contributed 90.5% in winter, 83.7% in the post monsoon season and 47.6% in summer. Similarly, Srivastava et al. [81] chemically analysed aerosols over Delhi in the IGP to identify their source, estimated the contribution of anthropogenic aerosols using the SBDART model in the year 2007, and found that the radiative forcing due to anthropogenic aerosols in winter was 90.7%, followed by post-monsoon season (84.3%) and summer (53.6%). Hence, based upon study results on seasonal variations in the contribution of anthropogenic aerosols in the IGP, the radiative forcing due to anthropogenic aerosols in winter, post-monsoon and summer (pre-monsoon and monsoon) is approximately 90%, 80% and 50%, respectively, that of radiative forcing due to aerosols under all-sky conditions (ARF_{all}) at the surface of the IGP. Therefore, seasonal radiative forcing due to anthropogenic aerosols under all-sky conditions ($AARF_{all}$) is given by

$$AARF_{all} = ARF_{all} \cdot \mu \tag{7}$$

where

μ = seasonal coefficient (value of μ for winter 0.9, post-monsoon 0.8, summer 0.5)

2.2.3. Crop Modelling

The crop model and the methodology adopted to simulate the effect of atmospheric aerosols on wheat production at the nodes of the study districts listed in Table 1 is described in the following subsections.

- Crop Model

In this study, the calibrated and validated APSIM model for SRFSI sites [70] is used to quantify the effect of atmospheric aerosols on crop production in the eastern IGP.

- Crop Simulation by APSIM

To quantify the effect of atmospheric aerosols on crop production, we used the already calibrated and validated APSIM rice-wheat cropping system [70]. This model was calibrated and validated using the SRFSI field trials data at the nodes listed in Table 1 from 2014 to 2017 in the eastern IGP [70]. Even though this calibrated and validated model is set up to evaluate conservation agriculture (CA) technologies across a range of cropping systems and locations in the eastern IGP, here, we used only one treatment of the model for the rice–wheat system with conventionally tilled puddled transplanted rice followed by conventionally tilled wheat, which is practiced by the majority of farmers in the eastern IGP.

In this study, we studied the impact of anthropogenic atmospheric aerosols on winter wheat in the eastern IGP. The amount of reduced radiation due to anthropogenic aerosols from 2014 to 2017 at the SRFSI nodes listed in Table 1 was estimated using Equation (7). The solar radiation without anthropogenic aerosols was estimated by adding this reduced solar radiation to the solar radiation observed for each day.

The alterations in energy balance due to anthropogenic aerosols also affects the ambient temperature globally [82]. Global models are used to study the implication of changes in temperature due to atmospheric aerosols; in this context, Freychet et al. [31] used the UK HadGEM Unified Model to study the local aerosol emission effect in North America, Europe, India and China from 1982 to 2016 and found that, in northeast India (i.e., eastern IGP), the maximum temperature was reduced by 0.5 °C during winter (December, January, and February). Here, it is assumed that the anthropogenic aerosols uniformly reduced the maximum temperature by 0.5 °C throughout the winter. Hence, the maximum temperature during winter months without anthropogenic aerosols is estimated by modifying the measured maximum temperature by adding 0.5 °C to each day. To study the impact of anthropogenic aerosols, simulation runs of the calibrated APSIM model at the SRFSI nodes were performed under three conditions: (1) with anthropogenic aerosol condition (no change in solar radiation and temperature); (2) without anthropogenic aerosol condition with only radiation effect; and (3) without anthropogenic aerosol condition with radiation and temperature effect. To minimize the effect of irrigation, automated irrigation is switched to 'on' mode with irrigation when available soil water fraction is below 0.5 in all simulations across all nodes. The APSIM simulation outputs at the SRFSI nodes are compared in terms of grain yield, biomass yield, and crop evapotranspiration.

2.2.4. Economic Loss and Gain Due to Anthropogenic Aerosols on Wheat Production

Data on the wheat-crop-cultivated area and production from the last five years in the Nepal, India and Bangladesh components of the eastern IGP were obtained from the corresponding national statistics. Based on the simulation results on the average gain or loss in wheat yield due to anthropogenic aerosols in the corresponding nodes in the eastern IGP, the gain or loss of wheat in each country component of the eastern IGP was obtained. By using the average wholesale price of wheat at Patna, a market at eastern IGP over the last 5 years (from April 2014 to April 2019), the total economic loss/gain due to anthropogenic aerosols on wheat production was assessed. Here, the economic losses and gains caused by the effect on biomass yield of wheat are not included in the analysis.

3. Results and Discussion

3.1. Atmospheric Aerosols in the Eastern IGP

The atmospheric aerosols in the eastern IGP were studied using historical AERONET data and field-measured particulate matter $PM_{2.5}$ data at eastern IGP stations. The average monthly distribution of AOD at 500 nm and the Angstrom Exponent measured at AERONET stations (Lumbini, Gandhi college, Dhaka and Bhola) in the eastern IGP are presented in Figures 4 and 5, respectively. It is evident from Figure 4 that, at all stations, the AOD is comparatively lower during monsoon season (June–September), which may be due to the wet scavenging of aerosols due to monsoon precipitation. However, AOD increases during the post-monsoon season at all stations and reaches its peak during winter months

(December–February), which is similar to the findings of Kumar et al. [5]. The increasing AOD during the post-monsoon season and the peak during the winter season are due to a combination of burning of agricultural residue along with other regular aerosols in those seasons and a shallow boundary layer during winter [4,8]. The Angstrom exponent at all stations, except Bhola, during the post-monsoon and winter season, is between 1.1 and 1.4, which indicates that the aerosol particle size is of mixed type (neither fine nor coarse), which is also in line with the findings of Kumar et al. [5]. The AOD pattern in the pre-monsoon season at two stations, Lumbini and Gandhi college, located in the western part of the eastern IGP, is distinctly different from the stations located in Bangladesh (Dhaka and Bhola), with an increasing AOD from March to June, which may be due to mineral dust transported from southwest Asia [83] being deposited before reaching the eastern area of the eastern IGP. This is supported by the comparatively low Angstrom exponent during pre-monsoon months at Gandhi college station in Figure 5. Similarly, a comparatively low Angstrom Exponent during monsoon months at Bhola (located adjacent to the Bay of Bengal) may be due to sea salts brought by the monsoon. From the distribution of AOD in the eastern IGP stations, it can be concluded that, except during monsoon season, in all months, the AOD is high, with a peak during winter in the eastern IGP, which may have strong implications for incoming solar radiation and winter crops due to the scattering and absorption of radiation in the atmosphere.
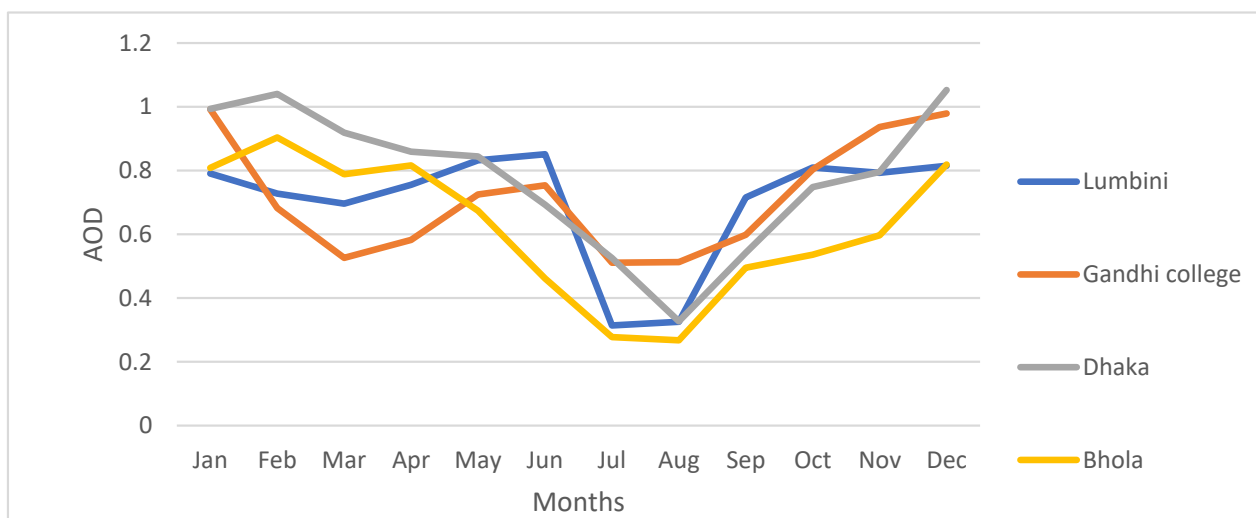
Figure 4. Average monthly distribution of AOD 500 nm based on AERONET data at eastern IGP.

The average monthly particulate matter ($PM_{2.5}$) measured [84] in several eastern IGP stations during 2018 is presented in Figure 6. The annual average $PM_{2.5}$ concentration of those stations is from 7 to 11 times higher than the World Health Organization (WHO) guideline of 10 μg m^{-3} [85]. The monthly distribution of particulate matter also shows a similar pattern to AOD, with a minimum during monsoon season and increase during the post-monsoon season, reaching a peak in the winter season and declining during pre-monsoon season. High particulate matter concentration during winter may be due to the increased use of biomass-based fuel for space heating. Moreover, in rural areas of northern India, cow dung cake is used as a residential fuel for cooking [86]. From biomass samples from IGP states of India, Singh et al. [87] found that dung cake produced comparatively more particulate matter than fuelwood and crop residue. Furthermore, Fosu et al. [88] found a strong relationship between particulate matter and atmospheric stability in the lower troposphere and increased aerosol loading during winter in the IGP, which was caused by the enhanced atmospheric stabilization during winter. Stations located in the western area of eastern IGP (viz. Gaya, Varanasi and Patna) show a hump in the month of June, which may be due to mineral dust transported from the western arid/desert regions of the Arabian Peninsula and the Thar Desert in India into the IGP [89]. The monthly

distribution of particulate matter in the eastern IGP shows critical air-quality conditions. The poor air quality is directly linked with negative implications for human health viz. increased risk of premature mortality, respiratory and cardiovascular diseases [90,91].
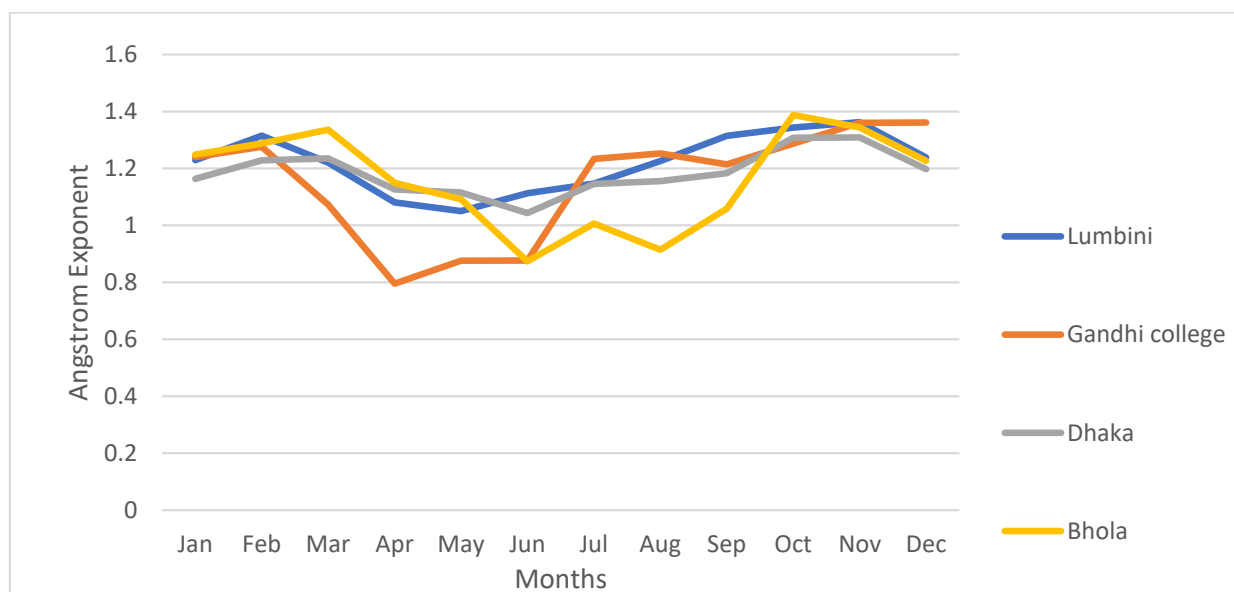
Figure 5. Average monthly distribution of Angstrom exponent (AE) based on AERONET data at eastern IGP.
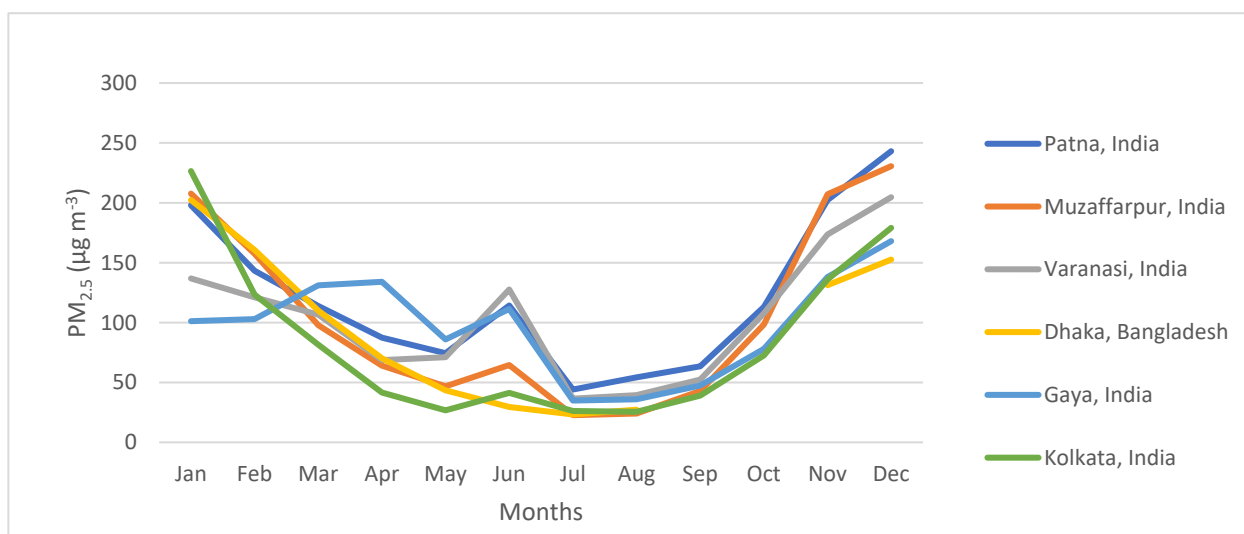
Figure 6. Monthly mean particulate matter distribution in eastern IGP during 2018.

3.2. Radiative Forcing Due to Atmospheric Aerosols in the Eastern IGP

The average seasonal radiative forcing during 2003–2017 due to anthropogenic aerosols, estimated by the method outlined in Section 2.2.2 at the SRFSI districts, is presented in Table 2. The table clearly indicates that compared to other seasons winter season radiative forcing is significantly higher in all the studied districts. High radiative forcing during winter is due to high anthropogenic aerosols in the eastern IGP. During monsoon season, the anthropogenic radiative forcing is minimal, which is due to the lower emissions of anthropogenic aerosols during monsoon season and wet scavenging of aerosols due to monsoon precipitation. In all the studied districts, the radiative forcing in the post-monsoon season is higher than that in pre-monsoon season due to a higher contribution of anthropogenic aerosols. Among the studied districts, the highest average radiative forcing is at

Rangpur, followed by Rajshahi and Purnea/Sunsari. The radiative forcing estimated at the SRFSI districts is comparable to the radiative forcing estimated by SBDART model at a station in eastern IGP, Gandhi college as -55.48 Wm^{-2} by using SBDART model [22].

Table 2. Radiative forcing due to anthropogenic aerosols (Wm^{-2}) in the SRFSI districts of eastern IGP.

SN	SRFSI Nodes in Eastern IGP	Pre-Monsoon	Monsoon	Post-Monsoon	Winter	Annual
1	Rangpur	−51.50	−33.26	−60.47	−107.35	−63.15
2	Rajshahi	−51.50	−30.57	−52.17	−88.68	−55.73
3	Purnea/Sunsari	−44.02	−18.23	−52.65	−84.42	−49.83

To obtain the seasonal and annual trends of anthropogenic radiative forcing in the studied districts in eastern IGP during 2003–2017, Mann–Kendall (MK) trend analysis is performed, and the results are presented in Table 3. From the MK trend analysis results, a significant declining trend in annual radiative forcing is found at all the studied districts, at least at the 0.01 level of statistical significance, during 2003–2017. The declining trend of radiative forcing in the SRFSI districts in the eastern IGP is due to the increasing levels of pollution and AOD during the study period. The rate of decline varied from 1.01 Wm^{-2} year^{-1} at Rajshahi to -1.5 Wm^{-2} year^{-1} at Rangpur during 2003–2017. Among the seasonal trends in radiative forcing, there is a significant decline in pre-monsoon season at all districts and in the winter season at Sunsari and Purnea district, at least at the statistically significant level of 0.05.

Table 3. Trends in seasonal and annual average radiative forcing due to atmospheric aerosols estimated during 2003–2017 at eastern IGP study sites.

SRFSI Districts at Eastern IGP	Seasonal/Annual	Test Z	Significance	Q	B
Rangpur	Pre-monsoon	−2.672	**	−1.279	−97.291
	Monsoon	−1.683	+	−0.908	−58.767
	Post Monsoon	−1.287		−1.379	−66.424
	Winter	−1.782	+	−1.644	−108.673
	Annual	−2.870	**	−1.508	−81.855
Rajshahi	Pre-monsoon	−2.573	*	−1.421	−96.719
	Monsoon	−1.881	+	−0.939	−55.164
	Post Monsoon	−0.891		−1.026	−55.422
	Winter	−1.386		−1.478	−85.368
	Annual	−2.969	**	−1.013	−76.012
Purnea/Sunsari	Pre-monsoon	−2.672	**	−1.485	−77.761
	Monsoon	−1.584		−0.929	−30.471
	Post Monsoon	−1.881	+	−1.050	−59.648
	Winter	−2.078	*	−2.106	−80.881
	Annual	−3.563	***	−1.209	−59.346

+ significant at 0.1, * significant at 0.05, ** significant at 0.01, *** significant at 0.001.

3.3. Solar Radiation Trend at the SRFSI Districts in Eastern IGP

Historical sunshine hour data of SRFSI district Sunsari in Nepal and Rajshahi in Bangladesh are used for a trend analysis of solar radiation. To obtain a monthly and annual trend of sunshine hours at Biratnagar, Sunsari, Nepal, from 1990 to 2016, the Mann—Kendall (MK) trend analysis was performed and the results are presented in Table 4.

The results indicate that the annual daily average sunshine hours are decreasing at the rate of 0.036 h (0.52%) per annum at a statistically significant level of 0.05 during those 26 years. This result agrees with the findings of Niroula et al. [92], who indicated surface dimming at a rate of −0.56% per annum in the Terai. Similarly, this is also in line with the findings of Kumari et al. [93], who found a 5% decline in solar radiation over the Indian region during 1980–2000. The increasing level of atmospheric aerosols contributed to the reduction in solar radiation in the Indian subcontinent, with pronounced effects in the IGP region [21,94–96]. The monthly trend results indicate that there is also a declining trend in sunshine hour at Biratnagar in all months, but the trend is only statistically significant in January, March, May, and December at the statistically significant level of 0.05. The rate of decline in December and January (winter months) is almost double that in the months of March and May (pre-monsoon months), which may be due to the increased level of aerosols and occurrence of fog events during winter months (December and January) in the Terai area of Nepal [97]. The sunshine hour trends at Biratnagar clearly indicate that significant surface dimming occurs at Biratnagar during winter months, which may affect the production of winter wheat [98].

Table 4. Trend of monthly and annual average daily sunshine hour from 1990 to 2016 at Biratnagar, Sunsari, Nepal.

Months	Test Z	Slope of a Trend Line, Q (h/year)	Intercept of a Trend Line, B (h)	Average Daily Sunshine Hour (h)	Interannual Trend of the Average Daily Sunshine Hour (%)
Jan	−3.045	−0.090 **	7.221	5.67	−1.59
Feb	−1.842	−0.041 +	7.999	7.17	−0.57
Mar	−2.538	−0.043 *	8.914	8.29	−0.52
Apr	−1.067	−0.025	8.888	8.33	−0.30
May	−2.030	−0.040 *	8.579	8.13	−0.49
Jun	−0.695	−0.031	6.510	6.27	−0.49
Jul	−0.630	−0.008	5.598	5.20	−0.16
Aug	−1.329	−0.054	6.476	5.65	−0.96
Sep	−0.755	−0.023	6.076	5.97	−0.38
Oct	−1.590	−0.036	8.214	7.50	−0.49
Nov	−1.072	−0.028	8.482	7.86	−0.36
Dec	−2.265	−0.082 *	7.689	6.49	−1.26
Annual	−2.360	−0.036 *	7.266	6.94	−0.52

+ significant at 0.1, * significant at 0.05, ** significant at 0.01.

Table 5 presents monthly and annual trend analysis results of sunshine hours at Rajshahi, Bangladesh during 1982–2017. The table clearly shows that sunshine hours are declining overall annually, as well as in the months of January, March, April, and December, at the statistically significant level of at least at 0.05 in Rajshahi, Bangladesh. The annual declining trend of daily sunshine hours at Rajshahi is 0.028 h per annum. Among the monthly trends, December and January have the largest declining trends, with 0.1 and 0.71 h/annum, respectively, compared to that of March and April, with declining trends of 0.24 and 0.026 h/annum, respectively. The high declining trend during winter months (December and January) compared to other months may be due to the increasing level of atmospheric aerosols [5,61] and fog events during winter [99] in the region. The trend analysis results indicate that surface dimming occurs at Rajshahi Bangladesh at a reduction rate in sunshine hours of 0.42% annually, with a very high reduction in winter months January and December of 1.09 and 1.46%, respectively. Similar to Biratnagar, Nepal, in Rajshahi, Bangladesh, winter crop production may also be affected by declining sunshine hours.

Table 5. Trends in the monthly and annual average daily sunshine hour from 1982 to 2017 at Rajshahi, Bangladesh.

Month	Test Z	Slope of a Trend Line, Q (h/year)	Intercept of Trend Line, B (h)	Average Daily Sunshine Hour (h)	Interannual Trend of the Average Daily Sunshine Hour (%)
Jan	−5.013	−0.071 ***	7.643	6.52	−1.09
Feb	−1.866	−0.030 +	8.665	7.95	−0.38
Mar	−2.465	−0.024 *	8.744	8.23	−0.29
Apr	−2.683	−0.026 **	8.503	8.05	−0.33
May	−1.131	−0.023	7.646	7.18	−0.31
Jun	−0.994	−0.015	5.312	5.26	−0.29
Jul	0.284	0.003	4.142	4.30	0.07
Aug	−0.852	−0.017	5.397	4.98	−0.35
Sep	0.852	0.019	5.267	5.52	0.34
Oct	−0.966	−0.016	7.687	7.20	−0.22
Nov	−1.562	−0.023	8.165	7.86	−0.29
Dec	−4.573	−0.100 ***	8.478	6.80	−1.46
Annual	−3.636	−0.028 ***	7.115	6.66	−0.42

+ significant at 0.1, * significant at 0.05, ** significant at 0.01, *** significant at 0.001.

3.4. Effect of Anthropogenic Atmospheric Aerosols on Wheat Production

The simulation results of APSIM on wheat production with and without anthropogenic aerosols at the SRFSI nodes in Nepal, India and Bangladesh are presented in this section. The effect of anthropogenic aerosols on wheat production is discussed in terms of wheat grain yield, wheat biomass yield, and total crop evapotranspiration.

3.4.1. Effect of Anthropogenic Atmospheric Aerosols on Wheat Production by Considering Only Solar Radiation Effect

The simulation results on wheat production with and without anthropogenic aerosols at the eastern IGP study nodes (listed in Table 1) when considering only the solar radiation effect are covered in this subsection.

- Effect on wheat yield

The APSIM simulation results for wheat grain yield with and without anthropogenic atmospheric aerosols during 2015–2017 at all the eastern IGP nodes are presented in Supplement Table S1. The simulation results indicate that anthropogenic aerosols reduce wheat grain yield in all the study nodes. The loss of wheat grain yield due to anthropogenic aerosols at the nodes ranges from 5.5% at Tikapatti to 22.2% at Bhaluwa. The reduction in wheat yield due to anthropogenic aerosols is in line with the findings of Liu et al. [53]. In addition, the decline in wheat yield under increased anthropogenic aerosols also agrees with the findings of Gupta et al. [45] and Burney and Ramanathan [44], based on statistical models in India. Countrywise, different wheat varieties were cultivated at the nodes in the eastern IGP. The variation in loss of wheat grain yield across the nodes of the eastern IGP could be due to the sensitivity of the cultivated wheat variety to the radiation changes along with the variations in soil type and meteorological parameters. The summarized countrywise effect on the wheat grain yield due to anthropogenic aerosols at the nodes of the eastern IGP is presented in Table 6. The table shows that, in all the country components of the eastern IGP, the average wheat grain yield is significantly reduced, ranging from 6.7% in India to 16.1% in Nepal. The average grain yield across the nodes in the eastern

IGP with and without anthropogenic aerosols is 3945.8 and 4560.8 kg/ha, showing a loss of 615 kg/ha (13.5%) on wheat yield during 2015–2017.

Table 6. Effect of anthropogenic aerosols (radiation only) on wheat grain yield in the eastern IGP.

Country Component of Eastern IGP	District	Nodes	Year	Grain Yield (kg/ha)		Gain/Loss of Grain Yield Due to Aerosols (+/−)	
				With Aerosols	Without Aerosols	(kg/ha)	(%)
Nepal	Sunsari	Bhaluwa and Simariya	2015–2016	3987.6	4751.4	−763.8	−16.1
India	Purnea	Tikapatti and Dogachhi	2015–2017	3832.2	4106.6	−274.4	−6.7
Bangladesh	Rajshahi and Rangpur	Baduria, Premtoli, Mohanpur and Kolkondo	2015–2017	3981.7	4692.6	−710.9	−15.1
Average of nodes in eastern IGP				3945.8	4560.8	−615.0	−13.5

The APSIM simulation results for wheat biomass yield with and without anthropogenic atmospheric aerosols during 2015–2017 at all the eastern IGP nodes are presented in Supplement Table S2. The results indicate that anthropogenic aerosols reduce wheat biomass yield at all the study nodes. Since APSIM calculates daily biomass production based on light interception and radiation use efficiency [98], the biomass yield in the IGP nodes declined with the anthropogenic aerosols due to a reduction in solar radiation. The loss of wheat biomass yield due to anthropogenic aerosols at the eastern IGP nodes ranges from 10.5% at Simariya and Dogachhi to 39.6% at Mohonpur. The variation in wheat biomass yield loss across the nodes of the eastern IGP could be due to the sensitiveness of cultivated wheat variety to the change in radiation, along with variations in soil type and meteorological parameters. It is observed that the comparatively higher biomass loss due to anthropogenic aerosols is observed at nodes in Bangladesh. The summarized countrywise effect on wheat biomass yield due to anthropogenic aerosols at the eastern IGP nodes is presented in Table 7. The table clearly shows that, in all the country components of the eastern IGP, the wheat biomass yield is significantly reduced, ranging from 11.5% at the nodes in Nepal and India to 31.4% in Bangladesh. The average biomass yield across the nodes in the eastern IGP with and without anthropogenic aerosols is 8280.5 and 10,610.3 kg/ha, which is a loss of 22% of wheat biomass yield during 2015–2017 due to the reduction in solar radiation. Since wheat straw is used as basal feed for dairy livestock in the IGP [100], the reduction in wheat biomass by anthropogenic aerosols might have affected its availability in the eastern IGP.

- Effect on wheat crop evapotranspiration

The simulation results on the effect of anthropogenic aerosols (by considering only the radiation effect) on wheat crop evapotranspiration at all the eastern IGP nodes during 2015–2017 are shown in Supplement Table S3. All nodes in the eastern IGP showed less crop evapotranspiration under anthropogenic aerosols due to the reduction in solar radiation. The decline in wheat crop evapotranspiration due to anthropogenic aerosols agrees with the findings of Yang et al. [98] and Yao [101]. The reduction in crop evapotranspiration varied from 5 percent at Bhaluwa, Nepal to 27.3 percent at Baduria, Bangladesh. The fluctuation in crop evapotranspiration reduction could be due to variations in wheat variety, soil, and meteorological parameters. Comparatively higher losses in crop evapotranspiration due to anthropogenic aerosols are observed in Bangladesh nodes in a similar manner as that of biomass yield loss in those nodes. The summarized country wise effect at the eastern IGP nodes on wheat crop evapotranspiration due to anthropogenic aerosols is presented

in Table 8. The table clearly shows that wheat crop evapotranspiration is significantly reduced in all the country component nodes of the eastern IGP, with reductions ranging from 5% at the nodes in Nepal to 20.3% at the nodes in Bangladesh. The average crop evapotranspiration across the nodes in the eastern IGP with and without anthropogenic aerosols are 269.6 and 311.6 mm, showing a loss of 13.5% in crop evapotranspiration during 2015–2017. The results show that the increased anthropogenic aerosols reduced the irrigation water demand of wheat in the eastern IGP.

Table 7. Effect of anthropogenic aerosols (radiation only) on wheat biomass yield in the eastern IGP.

Country Component of Eastern IGP	District	Nodes	Year	Biomass Yield (kg/ha)		Gain/Loss of Biomass Yield Due to Aerosols (+/−)	
				With Aerosols	Without Aerosols	(kg/ha)	(%)
Nepal	Sunsari	Bhaluwa and Simariya	2015–2016	9367.2	10,578.5	−1211.3	−11.5
India	Purnea	Tikapatti and Dogachhi	2015–2017	8486.1	9589.1	−1103.0	−11.5
Bangladesh	Rajshahi and Rangpur	Baduria, Premtoli, Mohanpur and Kolkondo	2015–2017	7634.4	11,136.8	−3502.4	−31.4
Average of nodes in eastern IGP				8280.5	10,610.3	−2329.8	−22.0

Table 8. Effect of anthropogenic aerosols (radiation only) on wheat evapotranspiration in the eastern IGP.

Country Component of Eastern IGP	District	Nodes	Year	Crop Evapotranspiration (mm)		Increase/Decrease on Crop Evapotranspiration (+/−) Due to Aerosols	
				With Aerosols	Without Aerosols	(mm)	(%)
Nepal	Sunsari	Bhaluwa and Simariya	2015–2016	295.3	310.9	−15.6	−5.0
India	Purnea	Tikapatti and Dogachhi	2015–2017	313.8	346.9	−33.1	−9.5
Bangladesh	Rajshahi and Rangpur	Baduria, Premtoli, Mohanpur and Kolkondo	2015–2017	234.6	294.3	−59.7	−20.3
Average of nodes in eastern IGP				269.6	311.6	−42.0	−13.5

3.4.2. Effect of Anthropogenic Atmospheric Aerosols on Wheat Production by Considering the Change in Solar Radiation and Maximum Winter Temperature

The simulation results of wheat crop performance with and without anthropogenic aerosols at the eastern IGP study nodes when considering the aerosol effects on daily solar radiation and maximum temperature is covered in this subsection. The effect on anthropogenic aerosols on wheat crop performance is discussed in terms of wheat grain yield, wheat biomass yield and crop evapotranspiration in the following subsections.

- Effect on wheat yield

The APSIM simulation results for wheat grain yield with and without anthropogenic atmospheric aerosols when considering the aerosol effects on daily solar radiation and

maximum temperature during 2015–2017 at all eastern IGP nodes are presented in Supplement Table S4. The simulation results indicate that anthropogenic aerosols reduce wheat grain yield in all study nodes except Simariya. The model indicated comparatively higher nitrogen stress of the wheat crop at Simariya, which could be due to comparatively poor soil fertility. The loss of wheat grain yield due to anthropogenic aerosols at the eastern IGP nodes ranges from −8.5% at Simariya to 22.3% at Bhaluwa. The variations in wheat grain yield response across the nodes could be due to the sensitivity of the cultivated wheat varieties to radiation and maximum temperature, along with variations in soil type, soil fertility, and meteorological parameters. The simulation results indicated that compared to the radiation only effect, the radiation and temperature (maximum) effect of anthropogenic aerosols have less loss in average grain yield in the eastern IGP nodes, and this result is supported by the findings of Rao et al. [102], who clearly indicated a negative correlation between maximum temperature and wheat yield in wheat-growing areas in India, including the IGP region. The summarized country wise effect on wheat grain yield due to anthropogenic aerosols at the nodes is presented in Table 9. The table clearly shows that, in all the country components of the eastern IGP, wheat grain yield is significantly reduced, ranging from 7% in India to 14% in Bangladesh. The average grain yield across the nodes in the eastern IGP with and without anthropogenic aerosols are 3945.8 and 4444.5 kg/ha, showing a loss of 498.7 kg/ha (11.2%) in wheat yield during 2015–2017.

Table 9. Effect of anthropogenic aerosols (radiation and maximum temperature) on wheat grain yield in the eastern IGP.

Country Component of Eastern IGP	District	Nodes	Year	Grain Yield (kg/ha)		Gain/Loss of Grain Yield Due to Aerosols (+/−)	
				With Aerosols	Without Aerosols	(kg/ha)	(%)
Nepal	Sunsari	Bhaluwa and Simariya	2015–2016	3987.6	4400.1	−412.4	−9.4
India	Purnea	Tikapatti and Dogachhi	2015–2017	3832.2	4122.4	−290.2	−7.0
Bangladesh	Rajshahi and Rangpur	Baduria, Premtoli, Mohanpur and Kolkondo	2015–2017	3981.7	4627.8	−646.1	−14.0
Average of nodes in eastern IGP				3945.8	4444.5	−498.7	−11.2

The simulation results for wheat biomass yield with and without anthropogenic atmospheric aerosols during 2015–2017 at all eastern IGP nodes when considering aerosol effects on daily solar radiation and maximum temperature are presented in Supplement Table S5. The results clearly indicate that anthropogenic aerosols reduce wheat biomass yield in all the study nodes. The loss of wheat biomass yield due to anthropogenic aerosols at the nodes ranges from 3.5% at Simariya to 38.9% at Mohonpur. The variation in wheat biomass yield loss across the nodes could be due to the sensitivity of the cultivated wheat varieties to radiation and maximum temperature, along with variations in soil type, fertility, and meteorological parameters. It is observed that a comparatively higher biomass is lost due to anthropogenic aerosols at nodes in Bangladesh. Overall, the reduction in biomass yield when considering the aerosol effects on radiation and temperature is slightly less than when considering the radiation-only effect in the eastern IGP (Supplement Tables S2 and S5). These results are in line with the findings of Asseng et al. [103] and Rao et al. [102], who clearly indicated a negative association between maximum temperature and wheat grain and biomass yield. The summarized countrywise effect on wheat biomass yield due to anthropogenic aerosols at the eastern IGP nodes is presented in Table 10. The table clearly shows that in all the country components of the eastern IGP the wheat biomass yield is

reduced significantly, ranging from 9.7 at the nodes in Nepal to 30.9 in Bangladesh. The average biomass yield across the nodes in the eastern IGP with and without anthropogenic aerosols are 8280.5 and 10,511.1 kg/ha, which shows a loss of 21.2% in wheat biomass yield during 2015–2017 due to the reduction in solar radiation and maximum temperature.

Table 10. Effect of anthropogenic aerosols (radiation and maximum temperature) on wheat biomass yield in the eastern IGP.

Country Component of Eastern IGP	District	Nodes	Year	Biomass Yield (kg/ha)		Gain/Loss of Biomass Yield Due to Aerosols (+/−)	
				With Aerosols	Without Aerosols	(kg/ha)	(%)
Nepal	Sunsari	Bhaluwa and Simariya	2015–2016	9367.2	10,375.0	−1007.8	−9.7
India	Purnea	Tikapatti and Dogachhi	2015–2017	8486.1	9563.7	−1077.6	−11.3
Bangladesh	Rajshahi and Rangpur	Baduria, Premtoli, Mohanpur and Kolkondo	2015–2017	7634.4	11,052.8	−3418.4	−30.9
Average of nodes in eastern IGP				8280.5	10,511.1	−2230.6	−21.2

- Effect on wheat crop evapotranspiration

The APSIM simulation results of the effect of anthropogenic aerosols, when considering their effects on solar radiation and maximum temperature, on wheat crop evapotranspiration at the eastern IGP nodes during 2015–2017, are shown in Supplement Table S6. All the nodes in the eastern IGP showed less crop evapotranspiration under anthropogenic aerosols due to the reduction in solar radiation and maximum temperature. The reduction in crop evapotranspiration varied from 8.4 percent at Simariya, Nepal to 27.7 percent at Baduria, Bangladesh. The variations in crop evapotranspiration reduction could be due to variations in the wheat variety, soil, and meteorological parameters. A comparatively higher loss in crop evapotranspiration due to anthropogenic aerosols is observed at Bangladesh nodes, in a similar manner as that of biomass yield loss in those nodes. These findings are supported by those of Zhang et al. [104], who showed a linear relationship between wheat biomass yield and evapotranspiration. The summarized countrywise effect at the eastern IGP nodes of the reduction in wheat crop evapotranspiration due to anthropogenic aerosols is presented in Table 11. The table clearly indicates that, in all the country components of the eastern IGP, wheat crop evapotranspiration is significantly reduced, ranging from 8.5% at the nodes in Nepal to 21.5% at the nodes in Bangladesh. The average crop evapotranspiration across the nodes in the eastern IGP with and without anthropogenic aerosols are 269.6 and 317.4 mm, which is a loss of 15.1% in crop evapotranspiration during 2015–2017.

Table 11. Effect of anthropogenic aerosols (radiation and maximum temperature) on wheat evapotranspiration in the eastern IGP.

Country Component of Eastern IGP	District	Nodes	Year	Crop Evapotranspiration (mm)		Increase/Decrease on Crop Evapotranspiration (+/−) Due to Aerosols	
				With Aerosols	Without Aerosols	(mm)	(%)
Nepal	Sunsari	Bhaluwa and Simariya	2015–2016	295.3	322.6	−27.3	−8.5
India	Purnea	Tikapatti and Dogachhi	2015–2017	313.8	349.4	−35.5	−10.2
Bangladesh	Rajshahi and Rangpur	Baduria, Premtoli, Mohanpur and Kolkondo	2015–2017	234.6	298.9	−64.3	−21.5
Average of nodes in eastern IGP				269.6	317.4	−47.9	−15.1

3.5. Loss Due to the Reduction in Wheat Yield

In this subsection, we estimate the loss of wheat production due to anthropogenic aerosols by considering the radiation only effect and the radiation and temperature effects in the eastern IGP region. The estimated loss in wheat production due to anthropogenic aerosols is presented in Table 12. The average area of wheat cultivated in the Nepal component, India component and Bangladesh component of the eastern IGP from 2011 to 2015 were 440,140, 2,447,580 and 402,940 Ha, respectively [105–107]. Average wheat cultivated area in the eastern IGP region is 3,290,660 ha. While considering only the radiation effect, the average model estimated yield reductions due to anthropogenic aerosols at the nodes in Nepal, India and Bangladesh are 0.764, 0.274, 0.711 t/ha, respectively (see Table 6). Similarly, when considering the solar radiation and temperature effect of anthropogenic aerosols, the average yield reduction estimated by the APSIM model at the nodes in Nepal, India and Bangladesh are 0.412, 0.290, 0.646 t/ha, respectively (see Table 9). The estimated wheat production reduction in the eastern IGP while considering only the radiation effect is 1293.39 thousand metric tons. While considering both the temperature and radiation effect, the reduction in wheat production by anthropogenic aerosols is estimated to be 1151.44 thousand metric tons. While considering the population of eastern IGP (361 million), the wheat production loss due to anthropogenic aerosols is estimated to be more than 3.2 kg of wheat per capita per annum during the study period. Given that the average wholesale price of wheat at Patna, a market in the eastern IGP from April 2014 to April 2019 is 262.50 USD/ton [108], then the total estimated loss in wheat production due to anthropogenic aerosols by considering only radiation effect is USD 339.52 million, whereas, when considering both radiation and temperature effect, the loss is USD 302.25 million. In summary, it is estimated that anthropogenic aerosols reduce wheat production in the eastern IGP by more than 1.1 million tons equivalent, which is worth more than USD 300 million. These values indicate that significant improvements in air quality could be achieved in the eastern IGP, even when only considering wheat production.

Generally, the cost of air pollution is estimated based on its negative effect on people's health. For example, the world bank estimated the cost of air pollution (welfare loss from air pollution) in several regions of the world, including South Asia, by considering the negative health effect on increased premature death and foregone labour output [109]. The report estimated welfare losses from ambient $PM_{2.5}$ in South Asia in the year 2013 as USD 256 billion. While comparing the cost of wheat production loss in the eastern IGP with the loss estimated by the World Bank group over the entire South Asia, it can be concluded that the economic loss of air pollution on agricultural production is significant and needs to be included when assessing the economic losses due to air pollution.

Table 12. Estimated loss in wheat production due to anthropogenic aerosols in the eastern IGP.

Country Component of Eastern IGP	Average Area * ('000 Ha)	Reduction in Wheat Yield Due to Atmospheric Aerosols while Considering		Estimated Wheat Production Reduced Due to Anthropogenic Aerosols while Considering		Estimated Loss [#] in Wheat Production Due to Anthropogenic Aerosols while Considering	
		Only Radiation Effect (T/ha)	Radiation and Temperature Effect (T/ha)	Only Radiation Effect ('000 T)	Radiation and Temperature Effect ('000 T)	Only Radiation Effect (Million USD)	Radiation and Temperature Effect (Million USD)
Nepal [1]	440.14	−0.764	−0.412	−336.27	−181.34	−88.27	−47.60
India [2]	2447.58	−0.274	−0.290	−670.64	−709.80	−176.04	−186.32
Bangladesh [3]	402.94	−0.711	−0.646	−286.49	−260.30	−75.20	−68.33
Eastern IGP	3290.66	−0.615	−0.499	−1293.39	−1151.44	−339.52	−302.25

* Based on 5 years (2011–2015) respective country statistics [105] [1], [106] [2] and [107] [3]. [#] Based on the average wholesale price of wheat (262.50 USD/ton) at Patna (eastern IGP) from April 2014 to April 2019.

4. Summary and Conclusions

In the context of persistently high levels of anthropogenic aerosols during winter in the eastern IGP, the present study examines the effect of anthropogenic aerosols on one of the important winter crops, wheat, using the process-based APSIM model. The APSIM model was calibrated and validated using data from the SRFSI project on-farm trials of rice-wheat cropping system at 8 nodes in the eastern IGP (4 in Bangladesh and 2 each in Nepal and India). The calibrated APSIM model was run with the observed meteorological data, which provides an estimate of wheat crop performance under anthropogenic aerosols at the eastern IGP nodes. Wheat crop performance without anthropogenic aerosols was obtained in two ways, first by running the model with adjusted observed solar radiation by estimating changed radiative forcing (considering only the radiative effect of anthropogenic aerosols), and second by running the model with adjusted solar radiation and maximum temperature data (considering the radiation as well as temperature effect of anthropogenic aerosols). The radiative effect of anthropogenic aerosols is estimated via the empirical model of clear-sky radiative forcing developed by Shrestha et. al. [77] and MERRA cloud fraction and cloud albedo over the SRFSI nodes and seasonal anthropogenic emission coefficients. In addition to the radiative effect, the temperature effect of anthropogenic aerosols in the eastern IGP was adapted in terms of a reduction of 0.5 °C on maximum temperature as suggested by Freychet et al. [31]. The impact of anthropogenic aerosols when considering only the radiative effect and the radiative and temperature effects was analysed at all 8 SRFSI nodes during 2015–2017. In addition, the aerosol loading, its trend, radiative forcing and the solar radiation trend at the study nodes were also analysed. The major findings of this study are listed below.

The analysis of AERONET AOD in the eastern IGP stations during 2003–2017 indicate that, in all months except during monsoon season, the average AOD of eastern IGP stations are high (greater than 0.5), with a peak during winter months. Annual mean particulate matter $PM_{2.5}$ at eastern IGP stations was found to be more than from 7 to 11 times higher than WHO guidelines. At all the stations in the eastern IGP, the monthly average particulate matter is increasing in post-monsoon months and reaches a peak during winter, which could be due to increased emissions from biomass burning, fossil fuel emissions, as well as enhanced atmospheric stabilization during winter months.

The estimated average annual radiative forcing due to anthropogenic aerosols at the SRFSI districts in the eastern IGP ranges from −49.83 to −63.15 Wm^{-2}. Regarding the seasonal distribution of radiative forcing, highest radiative forcing is observed during the winter season and the lowest radiative forcing is observed during monsoon season. Regarding the annual trend, all the SRFSI districts showed a statistically significant declining trend of radiative forcing during 2003–2017, at least at the statistical significance level of 0.01. The rate of decline varied from 1.01 Wm^{-2} $year^{-1}$ at Rajshahi to 1.5 Wm^{-2} $year^{-1}$ at Rangpur during 2003–2017. Regarding seasonal radiative forcing, pre-monsoon season

radiative forcing shows a declining trend in all SRFSI districts, at least at the statistical significance level of 0.05.

The historical trend of annual average sunshine hours at Sunsari and Rajshahi showed a declining trend at the rate of 0.42 and 0.52% per annum at least at the statistical significance level of 0.05. Regarding the monthly average trend in sunshine hours, both districts showed a statistically significant declining trend in the winter months of December and January at the rate of more than 1% per annum. The higher declining trend of sunshine hours during winter months could be due to an increased level of anthropogenic aerosols. Due to the high declining trend of sunshine hours during winter months, it is expected this will significantly affect winter crops.

The APSIM simulation results when only considering the radiative effect of anthropogenic aerosols indicate that the average grain yield loss in the eastern IGP is 615 kg/ha (13.5%). When considering both the radiative and temperature effects the simulation results showed the average loss of wheat grain yield at 498.7 kg/ha (11.2%) in the eastern IGP nodes. From these results, it can be concluded that anthropogenic aerosols result in significant grain yield loss at the range of 0.5 t/ha in the eastern IGP nodes. It is also revealed that the reduction in per capita wheat production due to anthropogenic aerosols in the eastern IGP is about 3.2 kg per annum. Hence, the substantial decline in wheat grain yield indicates a threat to the food security of the eastern IGP by anthropogenic aerosols (air pollution).

The APSIM model results also showed that anthropogenic aerosols significantly reduced biomass yield at all eastern IGP nodes. When considering the radiative-only and the radiative and temperature effects of anthropogenic aerosols, the average biomass yield in the eastern IGP nodes reduced by 22% and 21.2%, respectively. The reduction in biomass yield by the anthropogenic aerosols may also affect soil organic matter and animal fodder in the eastern IGP.

The APSIM model simulations when considering only the anthropogenic aerosols radiative effect reduced average wheat crop evapotranspiration by 42 mm (13.5%) at the eastern IGP nodes. When considering both radiative and temperature effects of anthropogenic aerosols, wheat crop evapotranspiration reduced by 47.9 mm (15.1%). Significant reductions in crop evapotranspiration due to anthropogenic aerosols, if considered during irrigation scheduling, may significantly save irrigation water.

By combining the average wheat yield loss from nodes in each country due to anthropogenic aerosols, average wheat-cultivated area in each country component of the eastern IGP, and the average wheat price for the study period, the estimated loss in wheat production due to anthropogenic aerosols was estimated in the eastern IGP. When considering only the radiative effect, wheat production loss caused by anthropogenic aerosols was estimated at USD 339.52 million in the eastern IGP per annum during 2015–2017. When considering both the radiative and temperature effects, wheat production loss caused by anthropogenic aerosols was estimated at USD 302.25 million in the eastern IGP per annum during 2015–2017. As the wheat production lost due to anthropogenic aerosols is found to be a significant, similar studies also need to be conducted for the other major crops in the eastern IGP to estimate the total economic loss from all crop production, which would make a significant contribution to assessing the economic loss due to air pollution in the eastern IGP.

5. Further Work Recommended

Crop simulation models, which are based on the concept of radiation-use efficiency (such as APSIM), require an input of daily values of *direct solar radiation* to simulate daily crop growth. The values for the radiation-use efficiency parameters used in these models vary with crop stage and include an implicit ratio of diffuse-to-direct radiation in their calibration. Although the models only use direct solar radiation as an input, the crops respond to both direct and diffuse components of the radiation [50,110]. The presence of aerosols is likely to increase the ratio due to increased light scattering [111–113] When aerosols are removed, the diffuse-to-direct radiation ratio will change, and there is a

possibility that the RUE values may be invalidated. A likely outcome would be the overestimation of crop production. In addition to the removals of aerosols, the effect of fog events and clouds during winter on direct and diffuse fraction (and, hence, on wheat production) should be investigated, as the significant reduction in solar radiation and subsequent reduction in daily maximum temperatures could also reduce the wheat yield in the eastern IGP ([114] in Bangladesh; [97] in Terai area of Nepal). This is a current research area and development in crop modelling, and we suggest that this analysis should be re-visited once the uncertainties are better understood.

Supplementary Materials: The following supporting information can be downloaded at: https://www.mdpi.com/article/10.3390/atmos13111896/s1, Table S1: Effect of anthropogenic aerosols on wheat grain yield in the eastern IGP; Table S2: Effect of anthropogenic aerosols on wheat biomass yield in the eastern IGP; Table S3: Effect of anthropogenic aerosols on wheat crop evapotranspiration in the eastern IGP; Table S4. Effect of anthropogenic aerosols on wheat grain yield in the eastern IGP; Table S5: Effect of anthropogenic aerosols on wheat biomass yield in the eastern IGP; Table S6: Effect of anthropogenic aerosols on wheat crop evapotranspiration in the eastern IGP.

Author Contributions: Conceptualization, S.S.; methodology, S.S.; formal analysis, S.S.; data curation, D.S.G., P.L.P. and S.K.D.; writing—original draft preparation, S.S.; writing—review and editing, M.C.P. and G.A.M.; visualization, S.S.; supervision, M.C.P., G.A.M., D.S.G. and P.L.P.; All authors have read and agreed to the published version of the manuscript.

Institutional Review Board Statement: Not applicable.

Informed Consent Statement: Not applicable.

Data Availability Statement: The datasets generated during and/or analyzed during the current study are available from the corresponding author on reasonable request.

Conflicts of Interest: The authors declare no conflict of interest.

References

1. Sen, A.; Abdelmaksoud, A.S.; Nazeer Ahammed, Y.; Alghamdi, M.O.; Banerjee, T.; Bhat, M.A.; Chatterjee, A.; Choudhuri, A.K.; Das, T.; Dhir, A.; et al. Variations in Particulate Matter over Indo-Gangetic Plains and Indo-Himalayan Range during Four Field Campaigns in Winter Monsoon and Summer Monsoon: Role of Pollution Pathways. *Atmos. Environ.* **2017**, *154*, 200–224. [CrossRef]

2. Wester, P.; Mishra, A.; Mukherji, A.; Shrestha, A.B.; Change, C. *The Hindu Kush Himalaya Assessment: Mountains, Climate Change, Sustainability and People*; Wester, P., Mishra, A., Mukherji, A., Shrestha, A.B., Eds.; International Center for Integrated Mountain Development (ICIMOD), Hindu Kush Himalayan Monitoring and Assessment Programme (HIMAP) and Springer Open: Kathmandu, Nepal, 2019; ISBN 9783319922874.

3. Mehta, M.; Singh, R.; Singh, A.; Singh, N. Anshumali Recent Global Aerosol Optical Depth Variations and Trends—A Comparative Study Using MODIS and MISR Level 3 Datasets. *Remote Sens. Environ.* **2016**, *181*, 137–150. [CrossRef]

4. Singh, N.; Mhawish, A.; Deboudt, K.; Singh, R.S.; Banerjee, T. Organic Aerosols over Indo-Gangetic Plain: Sources, Distributions and Climatic Implications. *Atmos. Environ.* **2017**, *157*, 69–74. [CrossRef]

5. Kumar, M.; Parmar, K.S.; Kumar, D.B.; Mhawish, A.; Broday, D.M.; Mall, R.K.; Banerjee, T. Long-Term Aerosol Climatology over Indo-Gangetic Plain: Trend, Prediction and Potential Source Fields. *Atmos. Environ.* **2018**, *180*, 37–50. [CrossRef]

6. David, L.M.; Ravishankara, A.R.; Kodros, J.K.; Venkataraman, C.; Sadavarte, P.; Pierce, J.R.; Chaliyakunnel, S.; Millet, D.B. Aerosol Optical Depth over India. *J. Geophys. Res. Atmos.* **2018**, *123*, 1–16. [CrossRef]

7. Srivastava, A.K.; Dey, S.; Tripathi, S.N. Aerosol Characteristics over the Indo-Gangetic Basin: Implications to Regional Climate. In *Atmospheric Aerosols—Regional Characteristics—Chemistry and Physics*; Abdul-Razzak, H., Ed.; InTech: London, UK, 2012; pp. 47–79, ISBN 978-953-51-0728-6.

8. Kumar, M.; Raju, M.P.; Singh, R.K.; Singh, A.K.; Singh, R.S.; Banerjee, T. Wintertime Characteristics of Aerosols over Middle Indo-Gangetic Plain: Vertical Profile, Transport and Radiative Forcing. *Atmos. Res.* **2017**, *183*, 268–282. [CrossRef]

9. Mao, K.B.; Ma, Y.; Xia, L.; Chen, W.Y.; Shen, X.Y.; He, T.J.; Xu, T.R. Global Aerosol Change in the Last Decade: An Analysis Based on MODIS Data. *Atmos. Environ.* **2014**, *94*, 680–686. [CrossRef]

10. TERI. *Air Pollutant Emissions Scenario for India*; Sharma, S., Kumar, A., Eds.; TERI: New Delhi, India, 2016; ISBN 9788179936399.

11. Paliwal, U.; Sharma, M.; Burkhart, J.F. Monthly and Spatially Resolved Black Carbon Emission Inventory of India: Uncertainty Analysis. *Atmos. Chem. Phys.* **2016**, *16*, 12457–12476. [CrossRef]

12. Sarkar, S.; Singh, R.P.; Chauhan, A. Crop Residue Burning in Northern India: Increasing Threat to Greater India. *J. Geophys. Res. Atmos.* **2018**, *123*, 6920–6934. [CrossRef]

13. Tiwari, S.; Hopke, P.K.; Thimmaiah, D.; Dumka, U.C.; Srivastava, A.K.; Bisht, D.S.; Rao, P.S.P.; Chate, D.M.; Srivastava, M.K.; Tripathi, S.N. Nature and Sources of Ionic Species in Precipitation across the Indo-Gangetic Plains, India. *Aerosol Air Qual. Res.* **2016**, *16*, 943–957. [CrossRef]

14. Pandey, S.K.; Vinoj, V.; Landu, K.; Babu, S.S. Declining Pre-Monsoon Dust Loading over South Asia: Signature of a Changing Regional Climate. *Sci. Rep.* **2017**, *7*, 1–10. [CrossRef] [PubMed]

15. Kaskaoutis, D.G.; Singh, R.P.; Gautam, R.; Sharma, M.; Kosmopoulos, P.G.; Tripathi, S.N. Variability and Trends of Aerosol Properties over Kanpur, Northern India Using AERONET Data (2001–10). *Environ. Res. Lett.* **2012**, *7*, 024003. [CrossRef]

16. Babu, S.S.; Manoj, M.R.; Moorthy, K.K.; Gogoi, M.M.; Nair, V.S.; Kompalli, S.K.; Satheesh, S.K.; Niranjan, K.; Ramagopal, K.; Bhuyan, P.K.; et al. Trends in Aerosol Optical Depth over Indian Region: Potential Causes and Impact Indicators. *J. Geophys. Res. Atmos.* **2013**, *118*, 11794–11806. [CrossRef]

17. Krishna Moorthy, K.; Suresh Babu, S.; Manoj, M.R.; Satheesh, S.K. Buildup of Aerosols over the Indian Region. *Geophys. Res. Lett.* **2013**, *40*, 1011–1014. [CrossRef]

18. WHO Ambient Air Quality Database, WHO. April 2018. Available online: http://www.who.int/airpollution/en/ (accessed on 20 March 2019).

19. Balakrishnan, K.; Dey, S.; Gupta, T.; Dhaliwal, R.S.; Brauer, M.; Cohen, A.J.; Stanaway, J.D.; Beig, G.; Joshi, T.K.; Aggarwal, A.N.; et al. Articles The Impact of Air Pollution on Deaths, Disease Burden, and Life Expectancy across the States of India: The Global Burden of Disease Study 2017. *Lancet Planet. Health* **2018**, *3*, e26–e39. [CrossRef]

20. Conibear, L.; Butt, E.W.; Knote, C.; Arnold, S.R.; Spracklen, D.V. Residential Energy Use Emissions Dominate Health Impacts from Exposure to Ambient Particulate Matter in India. *Nat. Commun.* **2018**, *9*, 1–9. [CrossRef]

21. Ramanathan, V.; Ramana, M.V. Persistent, Widespread, and Strongly Absorbing Haze over the Himalayan Foothills and the Indo-Gangetic Plains. *Pure Appl. Geophys.* **2005**, *162*, 1609–1626. [CrossRef]

22. Ramachandran, S.; Kedia, S. Radiative Effects of Aerosols over Indo-Gangetic Plain: Environmental (Urban vs. Rural) and Seasonal Variations. *Environ. Sci. Pollut. Res. Int.* **2012**, *19*, 2159–2171. [CrossRef]

23. Das, S.K.; Chatterjee, A.; Ghosh, S.K.; Raha, S. An Integrated Campaign for Investigation of Winter-Time Continental Haze over Indo-Gangetic Basin and Its Radiative Effects. *Sci. Total Environ.* **2015**, *533*, 370–382. [CrossRef]

24. Gilgen, H.; Wild, M.; Ohmura, A. Means and Trends of Shortwave Irradiance at the Surface Estimated from Global Energy Balance Archive Data. *J. Clim.* **1998**, *11*, 2042–2061. [CrossRef]

25. Wild, M. Global Dimming and Brightening: A Review. *J. Geophys. Res.* **2009**, *114*, 1–31. [CrossRef]

26. Singh, J.; Bhattacharya, B.K.; Kumar, M. Solar Radiation and Evaporation Trend over India. *Journal of Earth Science and Engineering* **2012**, *2*, 160–165.

27. Padmakumari, B.; Jaswal, A.K.; Goswami, B.N. Decrease in Evaporation over the Indian Monsoon Region: Implication on Regional Hydrological Cycle. *Clim. Chang.* **2013**, *121*, 787–799. [CrossRef]

28. Ramanathan, V.; Chung, C.; Kim, D.; Bettge, T.; Buja, L.; Kiehl, J.T.; Washington, W.M.; Fu, Q.; Sikka, D.R.; Wild, M. Atmospheric Brown Clouds: Impacts on South Asian Climate and Hydrological Cycle. *Proc. Natl. Acad. Sci. USA* **2005**, *102*, 5326–5333. [CrossRef]

29. Lau, K.M.; Kim, K.M. Observational Relationships between Aerosol and Asian Monsoon Rainfall, and Circulation. *Geophys. Res. Lett.* **2006**, *33*, 1–5. [CrossRef]

30. Meehl, G.A.; Arblaster, J.M.; Collins, W.D. Effects of Black Carbon Aerosols on the Indian Monsoon. *J. Clim.* **2008**, *21*, 2869–2882. [CrossRef]

31. Freychet, N.; Tett, S.F.B.; Bollasina, M.; Wang, K.C.; Hegerl, G.C. The Local Aerosol Emission Effect on Surface Shortwave Radiation and Temperatures. *J. Adv. Model. Earth Syst.* **2019**, *11*, 806–817. [CrossRef]

32. Gautam, R.; Hsu, N.C.; Kafatos, M.; Tsay, S.C. Influences of Winter Haze on Fog/Low Cloud over the Indo-Gangetic Plains. *J. Geophys. Res. Atmos.* **2007**, *112*, 1–11. [CrossRef]

33. Srivastava, S.K.; Sharma, A.R.; Sachdeva, K. Spatial and Temporal Variability of Fog Over the Indo-Gangetic Plains, India. *Int. J. Environ. Ecol. Eng.* **2016**, *10*, 1042–1057.

34. Singh, S.; Singh, D. Recent Fog Trends and Its Impact on Wheat Productivity in NW Plains in India. In Proceedings of the 5th International Conference on Fog, Fog Collection and Dew Münster, Münster, Germany, 25–30 July 2010.

35. Heagle, A.S.; Kress, L.W.; Temple, P.J.; Kohut, R.J.; Miller, J.E.; Heggestad, H.E. Factors Influencing Ozone Dose-Yield Response Relationships in Open-Top Field Chamber Studies. In *Assessment of Crop Loss from Air Pollution*; Heck, W.W., Taylor, O.C., Tingey, D.T., Eds.; Elsevier Appplied Science: London, UK; New York, NY, USA, 1987; pp. 141–180, ISBN 9789401071093.

36. Wahid, A.; Campus, Q. Effects of Air Pollution on Rice Yield in the Pakistan Punjab. *Environ. Pollut.* **1995**, *90*, 323–329. [CrossRef]

37. Maggs, R.; Wahid, A.; Shamsi, S.R.A.; Ashmore, M.R. Effects of Ambient Air Pollution on Wheat and Rice Yield in Pakistan. *Water Air Soil. Pollut.* **1995**, *85*, 1311–1316. [CrossRef]

38. Agrawal, M.; Singh, B.; Rajput, M.; Marshall, F.; Bell, J.N.B. Effect of Air Pollution on Peri-Urban Agriculture: A Case Study. *Environ. Pollut.* **2003**, *126*, 323–329. [CrossRef]

39. Hirano, T.; Kiyota, M.; Aiga, I. Physical Effects of Dust on Leaf Physiology of Cucumber and Kidney Bean Plants. *Environ. Pollut.* **1995**, *89*, 255–261. [CrossRef]

40. Przybysz, A.; Sæbø, A.; Hanslin, H.M.; Gawro, S.W. Accumulation of Particulate Matter and Trace Elements on Vegetation as Affected by Pollution Level, Rainfall and the Passage of Time. *Sci. Total Environ.* **2014**, *481*, 360–369. [CrossRef] [PubMed]

41. Weerakkody, U.; Dover, J.W.; Mitchell, P.; Reiling, K. Evaluating the Impact of Individual Leaf Traits on Atmospheric Particulate Matter Accumulation Using Natural and Synthetic Leaves. *Urban For. Urban Green.* **2018**, *30*, 98–107. [CrossRef]

42. Mina, U.; Chandrashekara, T.K.; Kumar, S.N.; Meena, M.C.; Yadav, S.; Tiwari, S.; Singh, D.; Kumar, P.; Kumar, R. Impact of Particulate Matter on Basmati Rice Varieties Grown in Indo-Gangetic Plains of India: Growth, Biochemical, Physiological and Yield Attributes. *Atmos. Environ.* **2018**, *188*, 174–184. [CrossRef]

43. Auffhammer, M.; Ramanathan, V.; Vincent, J.R. Integrated Model Shows That Atmospheric Brown Clouds and Greenhouse Gases Have Reduced Rice Harvests in India. *Proc. Natl. Acad. Sci. USA* **2006**, *103*, 19668–19672. [CrossRef]

44. Burney, J.; Ramanathan, V. Recent Climate and Air Pollution Impacts on India Agriculture. *Proc. Natl. Acad. Sci. USA* **2014**, *111*, 16319–16324. [CrossRef]

45. Gupta, R.; Somanathan, E.; Dey, S. Global Warming and Local Air Pollution Have Reduced Wheat Yields in India. *Clim. Chang.* **2017**, *140*, 593–604. [CrossRef]

46. Shuai, J.; Zhang, Z.; Liu, X.; Shi, Y.C.; Wang, P.; Shi, P. Increasing Concentrations of Aerosols Offset the Benefits of Climate Warming on Rice Yields during 1980–2008 in Jiangsu Province, China. *Reg. Environ. Chang.* **2013**, *13*, 287–297. [CrossRef]

47. Zhou, L.; Chen, X.; Tian, X. The Impact of Fi Ne Particulate Matter (PM 2.5) on China's Agricultural Production from 2001 to 2010. *J. Clean. Prod.* **2018**, *178*, 133–141. [CrossRef]

48. Bergin, M.H.; Ghoroi, C.; Dixit, D.; Schauer, J.J.; Shindell, D. Large Reductions in Solar Energy Production Due to Dust and Particulate Air Pollution. *Environ. Sci. Technol. Lett.* **2017**, *4*, 339–344. [CrossRef]

49. Chameides, W.L.; Yu, H.; Liu, S.C.; Bergin, M.; Zhou, X.; Mearns, L.; Wang, G.; Kiang, C.S.; Saylor, R.D.; Luo, C.; et al. Case Study of the Effects of Atmospheric Aerosols and Regional Haze on Agriculture: An Opportunity to Enhance Crop Yields in China through Emission Controls? *Proc. Natl. Acad. Sci. USA* **1999**, *96*, 13626–13633. [CrossRef] [PubMed]

50. Greenwald, R.; Bergin, M.H.; Xu, J.; Cohan, D.; Hoogenboom, G.; Chameides, W.L. The Influence of Aerosols on Crop Production: A Study Using the CERES Crop Model. *Agric. Syst.* **2006**, *89*, 390–413. [CrossRef]

51. Holzworth, D.P.; Snow, V.; Janssen, S.; Athanasiadis, I.N.; Donatelli, M.; Hoogenboom, G.; White, J.W.; Thorburn, P. Agricultural Production Systems Modelling and Software: Current Status and Future Prospects. *Environ. Model. Softw.* **2014**, *72*, 276–286. [CrossRef]

52. Gaydon, D.S.; Wang, E.; Poulton, P.L.; Ahmad, B.; Ahmed, F.; Akhter, S.; Ali, I.; Amarasingha, R.; Chaki, A.K.; Chen, C.; et al. Evaluation of the APSIM Model in Cropping Systems of Asia. *Field Crops Res.* **2017**, *204*, 52–75. [CrossRef]

53. Liu, X.; Sun, H.; Feike, T.; Zhang, X.; Shao, L.; Chen, S. Assessing the Impact of Air Pollution on Grain Yield of Winter Wheat—A Case Study in the North China Plain. *PLoS ONE* **2016**, *11*, 1–16. [CrossRef]

54. Xiao, D.; Tao, F. Contributions of Cultivars, Management and Climate Change to Winter Wheat Yield in the North China Plain in the Past Three Decades. *Eur. J. Agron.* **2014**, *52*, 112–122. [CrossRef]

55. Zhang, X.; Wang, S.; Sun, H.; Chen, S.; Shao, L.; Liu, X. Contribution of Cultivar, Fertilizer and Weather to Yield Variation of Winter Wheat over Three Decades: A Case Study in the North China Plain. *Eur. J. Agron.* **2013**, *50*, 52–59. [CrossRef]

56. Sun, H.; Zhang, X.; Wang, E.; Chen, S.; Shao, L.; Qin, W. Field Crops Research Assessing the Contribution of Weather and Management to the Annual Yield Variation of Summer Maize Using APSIM in the North China Plain. *Field Crops Res.* **2016**, *194*, 94–102. [CrossRef]

57. Xiao, D.; Tao, F. Contributions of Cultivar Shift, Management Practice and Climate Change to Maize Yield in North China Plain in 1981–2009. *Int. J. Biometeorol.* **2016**, *60*, 1111–1122. [CrossRef] [PubMed]

58. Sharma, B.; Amarasinghe, U.; Xueliang, C.; de Condappa, D.; Shah, T.; Mukherji, A.; Bharati, L.; Ambili, G.; Qureshi, A.; Pant, D.; et al. The Indus and the Ganges: River Basins under Extreme Pressure. *Water Int.* **2010**, *35*, 493–521. [CrossRef]

59. Taneja, G.; Pal, B.D.; Joshi, P.K.; Aggarwal, P.K.; Tyagi, N.K. *Farmerss Preferences for Climate-Smart Agriculture: An Assessment in the Indo-Gangetic Plain*; International Food Policy Research Institute (IFPRI): New Delhi, India, 2014.

60. Mamun, M.I.; Islam, M.; Mondol, P.K. The Seasonal Variability of Aerosol Optical Depth over Bangladesh Based on Satellite Data and HYSPLIT Model. *Am. J. Remote Sens.* **2014**, *2*, 20–29. [CrossRef]

61. Kar, J.; Deeter, M.N.; Fishman, J.; Liu, Z.; Omar, A.; Creilson, J.K.; Trepte, C.R.; Vaughan, M.A.; Winker, D.M. Wintertime Pollution over the Eastern Indo-Gangetic Plains as Observed from MOPITT, CALIPSO and Tropospheric Ozone Residual Data. *Atmos. Chem. Phys.* **2010**, *10*, 12273–12283. [CrossRef]

62. Erenstein, O.; Thorpe, W.; Singh, J.; Varma, A. *Crop–Livestock Interactions and Livelihoods in the Trans-Gangetic Plains, India*; ILRI: Nairobi, Kenya, 2007; ISBN 978-970-648-162-7.

63. Gupta, R.; Seth, A. A Review of Resource Conserving Technologies for Sustainable Management of the Rice-Wheat Cropping Systems of the Indo-Gangetic Plains (IGP). *Crop Prot.* **2007**, *26*, 436–447. [CrossRef]

64. Pal, D.K.; Bhattacharyya, T.; Srivastava, P.; Chandran, P.; Ray, S.K. Soils of the Indo-Gangetic Plains: Their Historical Perspective and Management. *Curr. Sci.* **2009**, *96*, 1193–1202.

65. Balasubramanian, V.; Adhya, T.K.; Ladha, J.K. Enhancing Eco-Efficiency in the Intensive Cereal-Based Systems of the Indo-Gangetic Plains. In *Eco-Efficiency: From Vision to Reality (Issues in Tropical Agriculture Series)*; Hershey, C.H., Neate, P., Eds.; International Center for Tropical Agriculture: Cali, Colombia, 2013; pp. 99–115, ISBN 9789586941181.

66. IndiaAgristat. Available online: https://www.indiaagristat.com (accessed on 24 January 2019).

67. CBS. *Statistical Pocket Book of Nepal 2014*; Central Bureau of Statistics, National Planning Commission Secretariat, Government of Nepal: Kathmandu, Nepal, 2014; ISBN 9789279483592.

68. Monlruzzaman; Rahman, M.S.; Karim, M.K.; Alam, Q.M. Agro Economic Analysis of Maize Production in Bangladesh: A Farm Level Study. *Bangladesh J. Agril. Res.* **2009**, *34*, 15–24. [CrossRef]

69. Gathala, M.K.; Tiwari, T.; Islam, S.; Maharjan, S.; Gerard, B. *Research Synthesis Report Sustainable and Resilient Farming Systems Intensification in the Eastern Gangetic Plains*; CIMMYT-ACIAR Publication: Canberra, Australia, 2018.

70. Gaydon, D.; Chaki, A.; Dutta, S.K.; Laing, A.; Poulton, P. *APSIM Modelling for On- Farm SRFSI Trials in the EGP*; CSIRO Publication: Melbourne, Australia, 2018.

71. Gilbert, R.O. *Statistical Methods for Environmental Pollution Monitoring*; Van Nostrand Reinhold Company: New York, NY, USA, 1987; ISBN 0471288780.

72. Sen, P.K. Estimates of the Regression Coefficient Based on Kendall's Tau. *J. Am. Stat. Assoc.* **1968**, *63*, 1379–1389. [CrossRef]

73. Lohmann, U.; Feichter, J. Global Indirect Aerosol Effects: A Review. *Atmos. Chem. Phys. Discuss.* **2004**, *4*, 7561–7614. [CrossRef]

74. Russell, P.B.; Hobbs, P.V.; Stowe, L.L. Aerosol Properties and Radiative Effects in the United States East Coast Haze Plume' An Overview of the Tropospheric Aerosol Radiative Forcing Observational Experiment. *J. Geophys. Res. Earth Surf.* **1999**, *104*, 2213–2222. [CrossRef]

75. Coakley, J.A.; Baldwin, D.G. Towards the Objective Analysis of Clouds from Satellite Imagery Data. *J. Clim. Appl. Meteorol.* **1984**, *23*, 1065–1099. [CrossRef]

76. Liu, Y.; Wu, W.; Jensen, M.P.; Toto, T. Relationship between Cloud Radiative Forcing, Cloud Fraction and Cloud Albedo, and New Surface-Based Approach for Determining Cloud Albedo. *Atmos. Chem. Phys.* **2011**, *11*, 7155–7170. [CrossRef]

77. Shrestha, S.; Peel, M.C.; Moore, G.A. Development of a Regression Model for Estimating Daily Radiative Forcing Due to Atmospheric Aerosols from Moderate Resolution Imaging Spectrometers (MODIS) Data in the Indo Gangetic Plain (IGP). *Atmosphere* **2018**, *9*, 405. [CrossRef]

78. Dey, S.; Tripathi, S.N.; Singh, R.P.; Holben, B.N. Influence of Dust Storms on the Aerosol Optical Properties over the Indo-Gangetic Basin. *J. Geophys. Res.* **2004**, *109*, 1–13. [CrossRef]

79. Jethva, H.; Satheesh, S.K.; Srinivasan, J. Seasonal Variability of Aerosols over the Indo-Gangetic Basin. *J. Geophys. Res. Atmos.* **2005**, *110*, 1–15. [CrossRef]

80. Dey, S.; Tripathi, S.N. Aerosol Direct Radiative Effects over Kanpur in the Indo-Gangetic Basin, Northern India: Long-Term (2001–2005) Observations and Implications to Regional Climate. *J. Geophys. Res. Atmos.* **2008**, *113*, 1–20. [CrossRef]

81. Srivastava, A.K.; Singh, S.; Tiwari, S.; Bisht, D.S. Contribution of Anthropogenic Aerosols in Direct Radiative Forcing and Atmospheric Heating Rate over Delhi in the Indo-Gangetic Basin. *Environ. Sci. Pollut. Res.* **2012**, *19*, 1144–1158. [CrossRef]

82. Shindell, D.T.; Lamarque, J.F.; Schulz, M.; Flanner, M.; Jiao, C.; Chin, M.; Young, P.J.; Lee, Y.H.; Rotstayn, L.; Mahowald, N.; et al. Radiative Forcing in the ACCMIP Historical and Future Climate Simulations. *Atmos. Chem. Phys.* **2013**, *13*, 2939–2974. [CrossRef]

83. Middleton, N.J. A Geography of Dust Storms in South—West Asia. *J. Climatol.* **1986**, *6*, 183–196. [CrossRef]

84. IQAir; AirVisual. *2018 World Air Quality Report Region and City PM 2.5 Ranking*; 2018. Available online: https://www.iqair.com/world-air-quality-report (accessed on 5 May 2019).

85. WHO. *Air Quality Guidelines for Particulate Matter, Ozone, Nitrogen Dioxide and Sulfur Dioxide: Global Update 2005: Summary of Risk Assessment*; WHO: Geneva, Switzerland, 2006.

86. Banerjee, T. Airing 'Clean Air' in Clean India Mission. *Environ. Sci. Pollut. Res.* **2017**, *24*, 6399–6413. [CrossRef]

87. Singh, D.P.; Gadi, R.; Mandal, T.K.; Saud, T.; Saxena, M.; Sharma, S.K. Emissions Estimates of PAH from Biomass Fuels Used in Rural Sector of Indo-Gangetic Plains of India. *Atmos. Environ.* **2013**, *68*, 120–126. [CrossRef]

88. Fosu, B.O.; Wang, S.Y.S.; Wang, S.H.; Gillies, R.R.; Zhao, L. Greenhouse Gases Stabilizing Winter Atmosphere in the Indo-Gangetic Plains May Increase Aerosol Loading. *Atmos. Sci. Lett.* **2017**, *18*, 168–174. [CrossRef]

89. Gautam, R.; Hsu, N.C.; Lau, K.M. Premonsoon Aerosol Characterization and Radiative Effects over the Indo-Gangetic Plains: Implications for Regional Climate Warming. *J. Geophys. Res. Atmos.* **2010**, *115*, 1–15. [CrossRef]

90. Schwartz, J.; Coull, B.; Laden, F.; Ryan, L. The Effect of Dose and Timing of Dose on the Association between Airborne Particles and Survival. *Environ. Health Perspect.* **2008**, *116*, 64–69. [CrossRef]

91. Brook, R.D.; Rajagopalan, S.; Iii, C.A.P.; Brook, J.R.; Bhatnagar, A.; Diez-roux, A.V.; Holguin, F.; Hong, Y.; Luepker, R.V.; Mittleman, M.A.; et al. Particulate Matter Air Pollution and Cardiovascular Disease An Update to the Scientific Statement From the American. *Circulation* **2010**, *21*, 2331–2378. [CrossRef]

92. Niroula, N.; Kobayashi, K.; Xu, J. Sunshine Duration Is Declining in Nepal across the Period from 1987 to 2010. *J. Agric. Meteorol.* **2015**, *71*, 15–23. [CrossRef]

93. Kumari, B.P.; Londhe, A.L.; Daniel, S.; Jadhav, D.B. Observational Evidence of Solar Dimming: Offsetting Surface Warming over India. *Geophys. Res. Lett.* **2007**, *34*, 1–5. [CrossRef]

94. Ramanathan, V.; Crutzen, P.J.; Lelieveld, J.; Mitra, P.; Althausen, D.; Anderson, J.; Andreae, M.O.; Cantrell, W.; Cass, G.R.; Chung, C.E.; et al. Indian Ocean Experiment: An Integrated Analysis of the Climate Forcing and Effects of the Great Indo-Asian Haze. *J. Geophys. Res.* **2001**, *106*, 28371. [CrossRef]

95. Dey, S.; Tripathi, S.N. Estimation of Aerosol Optical Properties and Radiative Effects in the Ganga Basin, Northern India, during the Wintertime. *J. Geophys. Res* **2007**, *112*, 1–16. [CrossRef]

96. Srivastava, R.; Ramachandran, S. The Mixing State of Aerosols over the Indo-Gangetic Plain and Its Impact on Radiative Forcing. *Q. J. R. Meteorol. Soc.* **2013**, *139*, 137–151. [CrossRef]

97. Shrestha, S.; Moore, G.A.; Peel, M.C. Trends in Winter Fog Events in the Terai Region of Nepal. *Agric. For. Meteorol.* **2018**, *259*, 118–130. [CrossRef]

98. Yang, X.; Asseng, S.; Wong, M.T.F.; Yu, Q.; Li, J.; Liu, E. Quantifying the Interactive Impacts of Global Dimming and Warming on Wheat Yield and Water Use in China. *Agric. For. Meteorol.* **2013**, *182–183*, 342–351. [CrossRef]

99. Syed, F.S.; Körnich, H.; Tjernström, M. On the Fog Variability over South Asia. *Clim. Dyn.* **2012**, *39*, 2993–3005. [CrossRef]

100. Erenstein, O. Cropping Systems and Crop Residue Management in the Trans-Gangetic Plains: Issues and Challenges for Conservation Agriculture from Village Surveys. *Agric. Syst.* **2011**, *104*, 54–62. [CrossRef]

101. Yao, L. Causative Impact of Air Pollution on Evapotranspiration in the North China Plain. *Environ. Res.* **2017**, *158*, 436–442. [CrossRef] [PubMed]

102. Rao, B.B.; Chowdary, P.S.; Sandeep, V.M.; Pramod, V.P.; Rao, V.U.M. Spatial Analysis of the Sensitivity of Wheat Yields to Temperature in India. *Agric. For. Meteorol.* **2015**, *200*, 192–202. [CrossRef]

103. Asseng, S.; Jamieson, P.D.; Kimball, B.; Pinter, P.; Sayre, K. Simulated Wheat Growth Affected by Rising Temperature, Increased Water Deficit and Elevated Atmospheric CO_2. *Field Crops Res.* **2004**, *85*, 85–102. [CrossRef]

104. Zhang, X.; Chen, S.; Sun, H.; Shao, L.; Wang, Y. Changes in Evapotranspiration over Irrigated Winter Wheat and Maize in North China Plain over Three Decades. *Agric. Water Manag.* **2011**, *98*, 1097–1104. [CrossRef]

105. MOAD. *Statistical Information of Nepalese Agriculture*; MOAD: Kathmandu, Nepal, 2018.

106. Datanet India Socio Economic Statistical Information about India. Available online: https://www.indiastat.com (accessed on 7 July 2018).

107. BBS. *45 Years Agriculture Statistics of Major Crops (Aus, Amon, Boro, Jute, Potato & Wheat)*; Bangladesh Bureau of Statistics (BBS), Statistical and Informatics Division (SID), Ministry of Planning, Government of Bangladesh: Dhaka, Bangladesh, 2018.

108. FAO Food Price Monitoring and Analysis. Available online: http://www.fao.org/giews/food-prices/tool/public/ (accessed on 9 May 2019).

109. World Bank Group; IHME. *The Cost of Air Pollution: Strengthening the Economic Case for Action*; World Bank Group: Washington, DC, USA, 2016.

110. Sinclair, T.R.; Shiraiwa, T.; Hammer, G.L. Variation in Crop Radiation-Use Efficiency with Increased Diffuse Radiation. *Crop Sci.* **1992**, *32*, 1281. [CrossRef]

111. Mercado, L.M.; Bellouin, N.; Sitch, S.; Boucher, O.; Huntingford, C.; Wild, M.; Cox, P.M. Impact of Changes in Diffuse Radiation on the Global Land Carbon Sink. *Nature* **2009**, *458*, 1014–1017. [CrossRef]

112. Zheng, B.Y.; Ma, Y.T.; Li, B.G.; Guo, Y.; Deng, Q.Y. Assessment of the Influence of Global Dimming on the Photosynthetic Production of Rice Based on Three-Dimensional Modeling. *Sci. China Earth Sci.* **2011**, *54*, 290–297. [CrossRef]

113. Li, T.; Heuvelink, E.; Dueck, T.A.; Janse, J.; Gort, G.; Marcelis, L.F.M. Enhancement of Crop Photosynthesis by Diffuse Light: Quantifying the Contributing Factors. *Ann. Bot.* **2014**, *114*, 145–156. [CrossRef] [PubMed]

114. Poulton, P.L.; Rawson, H.M.; Dalgliesh, N.P. Physical Constraints to Cropping in Southern Bangladesh. In *Sustainable Intensification of Rabi Cropping in Southern Bangladesh Using Wheat and Mung Bean*; Rawson, H.M., Ed.; ACIAR: Canberra, Australia, 2011; pp. 49–106.